#### Research Article

Muhammad Waqas Ashraf, Adnan Khan, Yongming Tu\*, Chao Wang\*, Nabil Ben Kahla, Muhammad Faisal Javed, Safi Ullah, and Jawad Tariq

# Predicting mechanical properties of sustainable green concrete using novel machine learning: Stacking and gene expression programming

https://doi.org/10.1515/rams-2024-0050 received May 15, 2024; accepted July 14, 2024

**Abstract:** Using rice husk ash (RHA) as a cement substitute in concrete production has potential benefits, including cement consumption and mitigating environmental effects. The feasibility of RHA on concrete strength was investigated in this research by predicting the split tensile strength (SPT) and flexural strength (FS) of RHA concrete (RHAC). The study used

\* Corresponding author: Yongming Tu, Key Laboratory of Concrete and Prestressed Concrete Structures of Ministry of Education, National Engineering Research Center for Prestressing Technology, School of Civil Engineering, Southeast University, 211189, Nanjing, China; Division of Structural and Fire Engineering, Department of Civil, Environmental and Natural Resources Engineering, Luleå University of Technology, SE-97187, Luleå, Sweden, e-mail: tuyongming@seu.edu.cn, yongmingtu@ltu.se

\* Corresponding author: Chao Wang, Division of Structural and Fire Engineering, Department of Civil, Environmental and Natural Resources

Engineering, Department of Civil, Environmental and Natural Resources Engineering, Luleå University of Technology, SE-97187, Luleå, Sweden, e-mail: chao.wang@ltu.se

**Muhammad Waqas Ashraf:** Key Laboratory of Concrete and Prestressed Concrete Structures of Ministry of Education, National Engineering Research Center for Prestressing Technology, School of Civil Engineering, Southeast University, 211189, Nanjing, China

**Adnan Khan:** School of Transportation, Southeast University, Jiulonghu Campus, Jiangning District, Nanjing, Jiangsu, 211189, China

**Nabil Ben Kahla:** Department of Civil Engineering, College of Engineering, King Khalid University, PO Box 394, Abha, 61411, Saudi Arabia; Center for Engineering and Technology Innovations, King Khalid University, Abha, 61421, Saudi Arabia

**Muhammad Faisal Javed:** Department of Civil Engineering, COMSATS University Islamabad, Abbottabad Campus, Islamabad, Pakistan; Department of Technical Science, Western Caspian University, Baku, Azerbaijan

Safi Ullah: Key Laboratory of Concrete and Prestressed Concrete Structures of Ministry of Education, National Engineering Research Center for Prestressing Technology, School of Civil Engineering, Southeast University, 211189, Nanjing, China; Department of Construction Management, Global Banking School (Bath Spa University), Devonshire Street North, Manchester, M12 6JH, United Kingdom Jawad Tariq: School of Civil Engineering, Henan University of Technology, Zhengzhou, Henan, 450001, China

machine learning (ML) methods such as ensemble stacking and gene expression programming (GEP). The stacking model was improved using base learner configurations ML models, such as, random forest (RF), support vector regression, and gradient boosting regression. The proposed models were validated by statistical tests and external validation criteria. Moreover, the effect of input parameters was investigated using Shapley adaptive exPlanations (SHAP) for RF and parametric analysis for GEP-based models. The analysis revealed that the stacking ensemble integrates base learner predictions and demonstrated superior performance, with R values greater than 0.98 and 0.96. Mean absolute error and root mean square error values for both SPT and FS were 0.23, 0.3, 0.5, and 0.7 MPA, respectively. The SHAP analysis demonstrated water, cement, superplasticizer, and age as influential parameters for the RHAC strength. Furthermore, the SPT and FS of RHAC can be predicted with an acceptable error using the GEP expressions in the standard design procedure.

**Keywords:** rice husk ash, stacking, gene expression programming, tensile and flexural strength, parametric analysis, SHAP analysis

### 1 Introduction

The construction industry prioritizes sustainable materials, particularly concrete, which is a high-energy and resource-intensive material. Consequently, researchers are exploring alternatives to traditional cement and components that minimize environmental impact. Rice husk ash (RHA), a readily available by-product from rice milling, holds promise as a sustainable concrete constituent [1]. The finished product, known as husk, is contained within the rice grain. In the paddy production cycle, 78% of the weight is received as rice and 22% is husk [2]. Approximately 750 million tons of rice husk are produced worldwide every year [3]. The research concludes that RHA consists of 85–95% amorphous silica [4]. However, this silica is not biodegradable and is

commonly utilized in landfills. It is widely recognized that RHA has both filler and pozzolanic effects in mortar and concrete. The effects of RHA varied among samples due to factors such as paddy type, crop year, climate, and location [5]. Researchers found that RHA's silica generation, carbon reduction, structure, fineness, ignition loss, increasing filler, and pozzolanic activity are influenced by incineration technique, temperature, and burning time [6]. There have been several attempts to develop and utilize RHA in practical research. According to reports, concrete's pozzolanic and filler action with RHA results in notable microstructural changes [6–8].

The incorporation of RHA in concrete offers a promising approach to enhance its properties, including compressive strength (CS), split tensile strength (SPT), and durability, as demonstrated by numerous research studies. RHA not only improves concrete performance but also reduces material costs due to decreased cement demand. Additionally, it provides environmental benefits through effective waste management [9]. Chopra and Siddique [4] investigated concrete strength at various ages using RHA substitute proportions of 0, 10, 15, and 20%. Results indicate a 25, 33, and 36% improvement in concrete CS at 7, 28, and 56 days at a 15% substitution rate; similarly, cement replacement with RHA increased SPT by 15%. Singh [10] concluded that SPT increased by 3.9% with 5% replacement but decreased by 17.5% at 10% replacement. Likewise, flexural strength (FS) increased by 10.9% at 5% replacement but decreased by 3% at 10% replacement compared to the control mix. Over 10% replacement, SPT and FS decreased significantly, with 19.3% SPT decrease at 15% replacement and 31.7% SPT decrease at 20% replacement. The study observed that the highest CS, SPT, and FS values were achieved after 7, 14, and 28 days of curing when the RHA was replaced by 15%. Additionally, it was found that the percentage loss of strength and weight increased as the content of RHA increased from 0 to 25% [11]. Several types of factors can be influenced by using RHA as supplementary cementation material, including the aggregate water-tocement ratio, particle size, waste content, and compressive loading ability [12]. Furthermore, using these materials in concrete enhances its ability to withstand compression, decreases its emission of greenhouse gases, and improves its SPT and FS, as depicted in Figure 1.

Although mechanical testing is the most typical method for evaluating concrete's CS and SPT, it tends to be time-consuming and expensive [2]. Some researchers have developed a linear regression (LR) model to predict the SPT and FS of concrete. However, due to the quite nonlinear relationships between the concrete components and strength, it is challenging to develop accurate predictions [13]. Researchers have

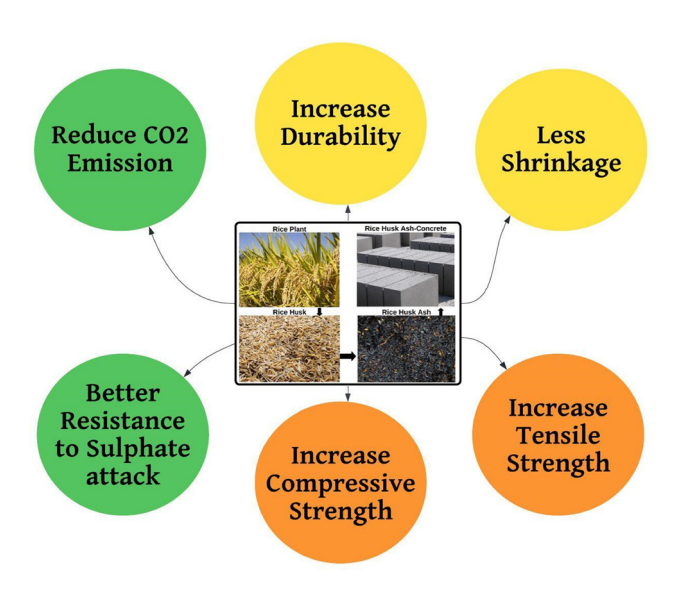


Figure 1: Manufacturing and effect of RHA concrete.

turned to artificial intelligence (AI) algorithms to address structural challenges [14]. AI techniques such as artificial neural networks (ANNs) are a pattern recognition system that determines the pattern between different parameters, a computational approach that is increasingly used in developing predictive models [15,16]. Another advantage of AI, in contrast to traditional regression techniques, is superior performance, and it can handle complex data and nonlinear relationships between independent and dependent parameters. Therefore, several studies have leveraged AI techniques to predict CS. Among the prevalent AI methods for analyzing concrete properties are ANN and support vector machines (SVM) [17]. Recently, a high-performance concrete strength prediction model was developed using a modified firefly approach combined with an ANN model, showcasing impressive predictive capabilities [18]. Such algorithms play a pivotal role in enhancing the design and performance of concrete mixes [19,20]. Another study also used the ANN approach to predict the CS of lightweight concrete reinforced with steel fibers [21]. Similarly, the ANN model is an effective methodology for predicting the mechanical properties of sustainable concrete [22-25]. Furthermore, ANNs have been observed to have limited external validity when employed in analyzing diverse datasets. Additionally, it is difficult to determine the optimal architecture of neural networks and the number of hidden layers in the structure. To address the aforementioned issues inherent to ANNs, it is essential to provide adequate attention to tree-based ensemble approaches. Ensemble learning approaches have become increasingly popular due to their greater prediction capabilities [26–28]. Some researchers have proposed bagging and boosting series algorithms for concrete strength prediction.

To predict concrete strength, Lyngdoh et al. used significant machine learning (ML) algorithms. According to their outcomes, the XGBoost model is the most effective [29]. In another study, XGBoost and CatBoost were employed to predict the concrete strength, and it was discovered that XGBoost and CatBoost had considerably fewer mean errors between predicted and actual values [30]. Hybrid ML models were used to predict the strength of ultra-high-performance concrete and were found to have a better-predicted performance than traditional methods [31,32]. Gene expression programming (GEP) algorithm, simple and practical mathematical equations predicted ground granulated blast-furnace slag (GGBS)-based geopolymer concrete mortar CS [33]. Chu et al. [34] concluded that the accuracy and predictability of GEP and multi-expression programming (MEP) models were evaluated by comparing them with LR and nonlinear regression (NLR) models. The GEP equation demonstrated a diminished statistical error and a higher correlation coefficient than the MEP equation. Moreover, Table 1 summarizes the prediction properties presented by various researchers.

While ensemble and boosting techniques have been established as efficient modeling methodologies across various engineering applications, there remains a limited exploration of these techniques for SPT and FS [35-37]. In addition, very little scientific research has been done on using stacking ensemble techniques to predict the mechanical properties of RHA concrete (RHAC). The advantage of the stacking ensemble model is that it combines the best

prediction models and achieves robust prediction results. Therefore, in this study, stacking-based ensemble models are created to predict the mechanical properties (SPT, FS) of RHAC. Ensemble learning models were utilized for base learners. For individual prediction and model hyperparameter optimization, random forest (RF), support vector regression (SVR), and gradient boosting regression (GBR) were employed. The stacking ensemble learning model has been developed employing LR as the meta-learners and RF and/or SVR and GBR models as the base learners. In addition, GEP models have been developed to establish empirical relationships with acceptable error margins for predicting SPT and FS. Furthermore, various statistical criteria, interpretations, and parametric analyses validated the models' effectiveness.

# 2 Research methodology

## 2.1 Data acquisition

In ML-based prediction models, the greater range of data with stronger correlation and accurate choice of input variables can help create a more valuable model with higher accuracy. In this regard, the models were developed using a comprehensive database of RHAC sourced from existing literature [4,10,50-59]. This database comprises

Table 1: Existing research summary of ML algorithm for sustainable concrete

Ref.	ML algorithm	Dataset size	Material	Investigated property
[35]	DT, RF, SVM, K-nearest neighbors, and ANN	625	GGBFS	CS
	-			
[38]	Adaptive regression splines (MARS)	161	GGBFS	CS
[39]	Multilayer perceptron neural network (MLPNN) and	145	Alkali activated	Statistic and dynamic yield stress
	bagging ensemble (BE)		concrete (AAC)	
[40]	MLPNN, bagging, and XGB	676	AAC	CS
[34]	GEP and MEP	311	Fly-ash (FA)	CS
[36]	SVM and gradient boosting machine (GBM)	81	Ceramic waste and	SPT and CS
			nylon fiber	
[41]	MARS, GEP, M5P Model Tree (M5P) and extreme learning	449	Oil palm by-product	CS
	machine (ELM)		. , , ,	
[42]	XGBoost, AdaBoost, and DT	60	Ceramic waste powder	CS
[37]	SVM	115	FA	CS
[43]	MARS	21	Crumb rubber with	CS
			Silica fume	
[44]	ANN, GP, M5P, SVM	137	Waste foundry sand (WFS)	CS, SPT, and FS
[45]	ANN	470, 295	WFS	CS, SPT, FS, modulus of elasticity
[46]	LR, Multilinear regression, NLR	420	Nanosilica	CS
[47]	LGB, XGB, RF	1,404	RHAC	CS
[48]	ANN	236	FA	CS
[49]	Neuro-imperialism and neuro-swarm)	379	FA	CS

110 and 67 data points for SPT and FS, respectively. In addition, the collected data sample experiments were carried out according to the ASTM and IS standards. For modeling SPT and FS, the independent variables included cement (C), water (W), fine aggregate (FA), RHA, SP, and age. Table 2(a) and (b) illustrates the characterizations of the comprehensive data employed for developing the models. Furthermore, the model is expected to perform optimally due to the extensive distribution of the independent variables. For clear model interpretation, it is essential to understand the interactions between the model's parameters. This correlation among specific components is termed multi-collinearity. In this study, ensuring a correlation value below 0.8 between pertinent variables will mitigate this issue, positively influencing the model's construction. The correlation matrix of the dataset is presented in Figure 2(a) and (b).

#### 2.2 Methods

ML methods can be categorized based on their learning type, such as supervised, unsupervised, and reinforcement learning. Regarding the known objective feature in this study, only the supervised approach was employed. Supervised learning is an approach employed in the development of ML models, where a computer algorithm is trained using input data that has been annotated with specific output labels.

This section describes several supervised ML approaches, namely SVR, RF, GBR, and GEP. The main distinctness of this study is the development of a stacking model that integrates numerous algorithms for ML, based on a metamodel, to attain the utmost accuracy in prediction. The research methodology flowchart can be seen in Figure 3.

#### 2.2.1 RF

The RF algorithm was developed as a robust ensemble learning technique based on classification and regression trees. The initial RF-based technique was introduced in 1995, and afterward, an improved version was published by Breiman [60]. The application of RF algorithms has been extensively utilized across various domains, demonstrating outstanding performance, particularly in tasks including classification and regression is a statistical learning theory-based methodology that uses the bootstrap resampling technique to extract multiple samples from the original data [47]. This technique is employed before modeling the decision tree (DT) for each bootstrap sample. Ultimately, the forecasts generated by the different DTs are aggregated and averaged to obtain the ultimate prediction outcome, as shown in Figure 4, which also represents the graphical view of the RF algorithm. The RF algorithm enhances the diversity of DTs by enabling the use of replacement samples and introducing random variations in

Table 2: Data descriptive statistics for SPT and FS

Statistics parameters	<i>C</i> (kg·m <sup>-3</sup> )	W (kg·m <sup>-3</sup> )	FA (kg·m <sup>-3</sup> )	RHA (kg·m <sup>-3</sup> )	SP (kg·m <sup>−3</sup> )	Age (days)	Strength (MPa)
(a) SPT							
Minimum	36.80	112.50	482.46	0.00	0.00	7.00	1.39
Mean	360.20	183.12	618.00	46.62	3.34	22.27	3.55
Maximum	550.00	238.00	910.00	165.00	15.00	28.00	8.10
Range	513.20	125.50	427.54	165.00	15.00	21.00	6.71
Standard error	6.46	3.25	11.12	3.45	0.36	0.90	0.16
Standard deviation	67.72	34.07	116.64	36.20	3.59	9.40	1.70
Sample variance	4586.65	1160.52	13604.73	1310.74	12.92	88.27	2.90
Kurtosis	4.83	-0.98	0.55	0.15	4.32	-0.95	0.10
Skewness	-0.15	-0.03	1.02	0.63	1.97	-1.03	1.00
(b) FS							
Minimum	36.80	112.50	492.58	0.00	0.00	7.00	1.20
Mean	358.18	177.53	596.73	48.19	2.36	22.36	5.76
Maximum	550.00	238.00	750.00	165.00	6.75	28.00	14.10
Range	513.20	125.50	257.42	165.00	6.75	21.00	12.90
Standard error	8.21	4.42	9.47	4.68	0.25	1.15	0.36
Standard deviation	67.22	36.14	77.54	38.33	2.07	9.38	2.97
Sample variance	4517.95	1306.43	6012.74	1469.56	4.29	87.96	8.81
Kurtosis	7.56	-0.84	-0.62	0.28	0.04	-0.89	1.54
Skewness	-1.14	0.19	0.52	0.66	0.79	-1.07	1.28

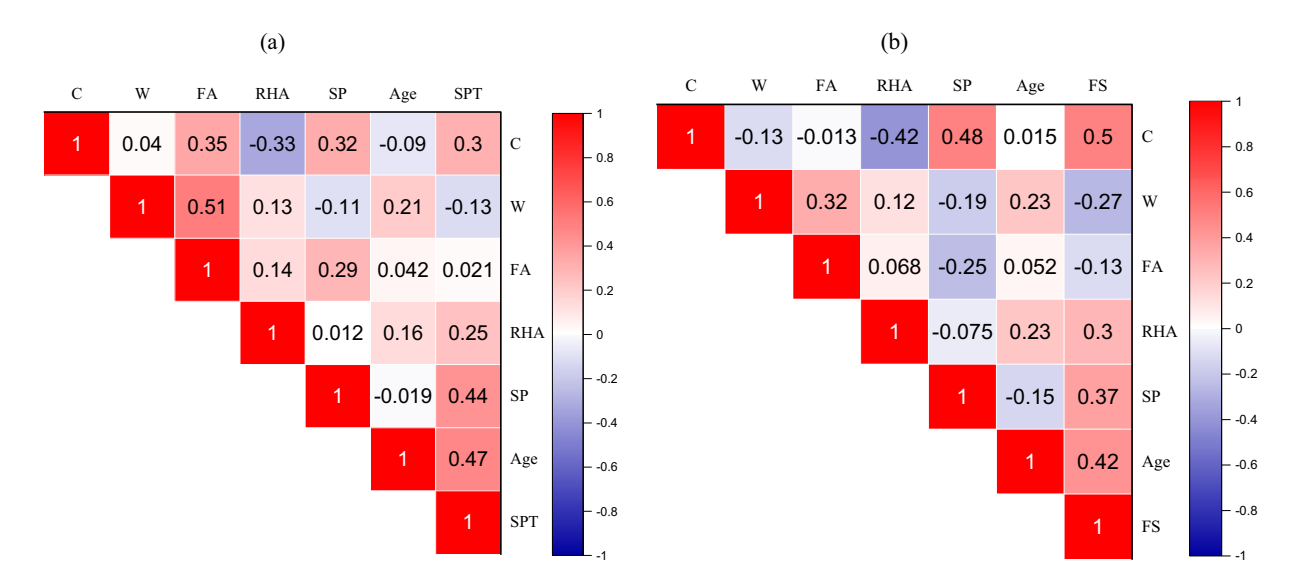


Figure 2: Correlation metrics between input and output of (a) SPT and (b) FS.

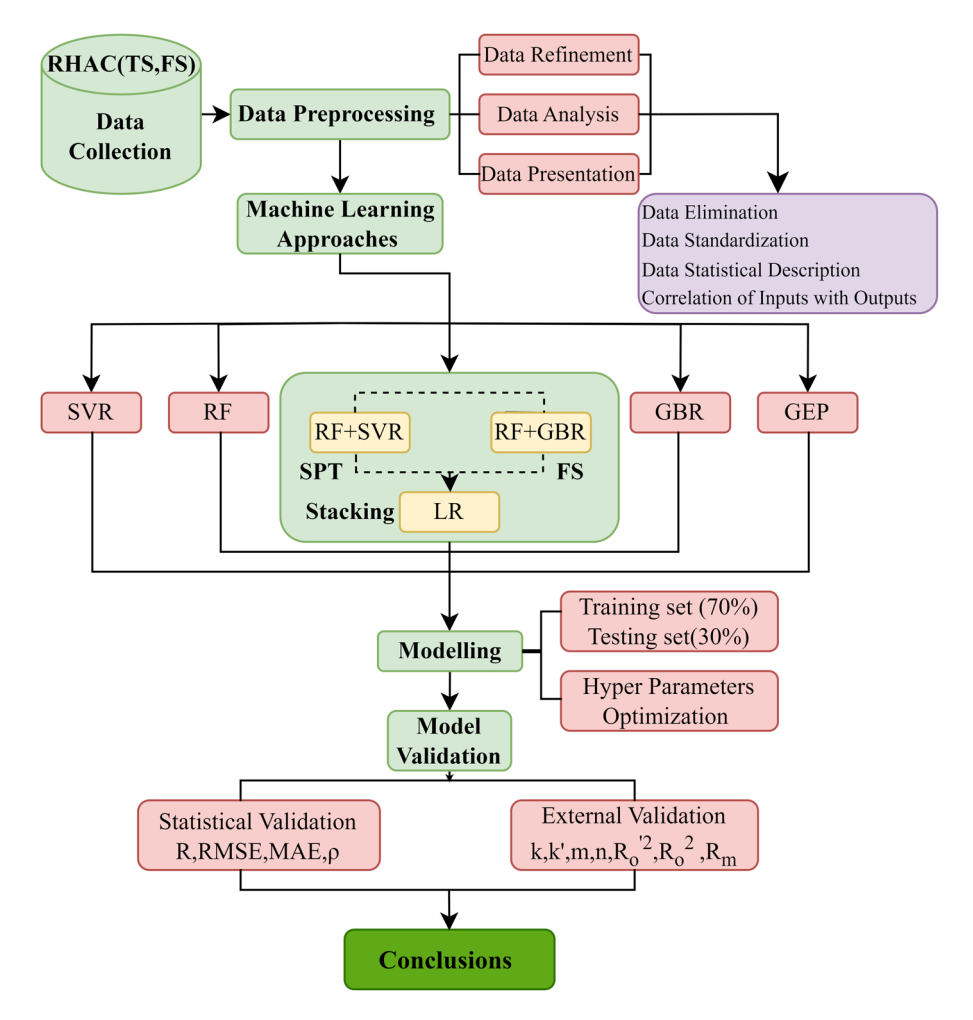


Figure 3: Research methodology flowchart.

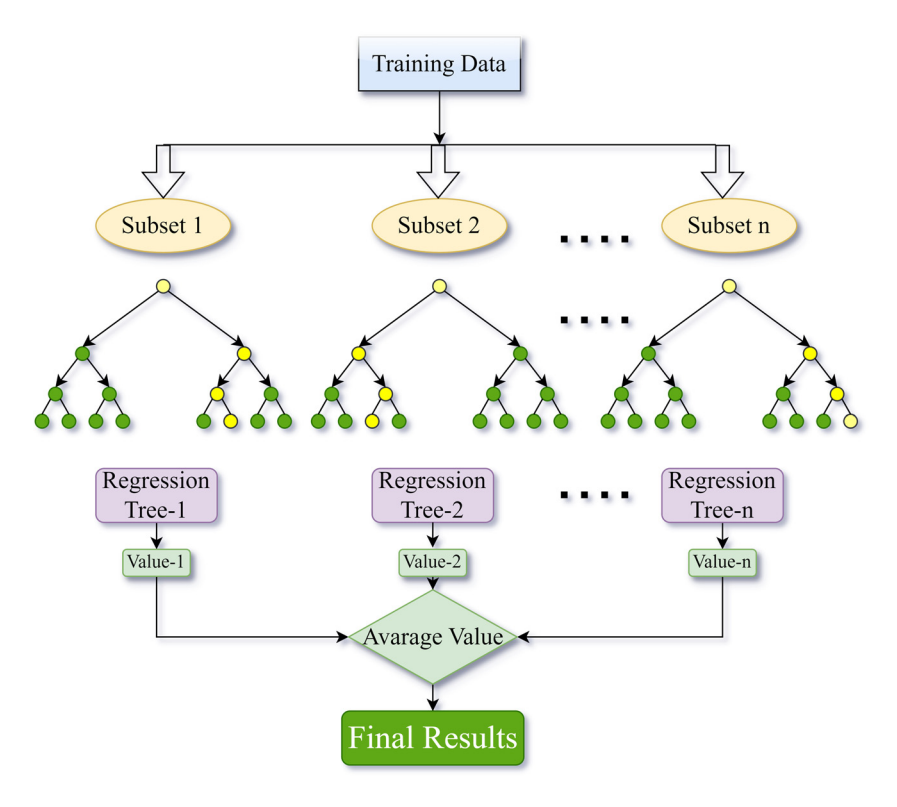


Figure 4: Schematic view of RF.

predictor combinations during the evolution of distinct trees. Further details can be obtained in [61].

#### 2.2.2 SVR

Vapnik [62] pioneered the SVM algorithm as a means of addressing classification issues, and it was subsequently extended to include the fixing of regression problems. The SVM algorithm implements the principle of structural risk minimization (SRM), which has been demonstrated to be more effective [63] compared to the usual empirical risk minimization (ERM) principle. The SRM approach aims to reduce a limit on the predicted risk, in contrast to the ERM approach, which focuses on minimizing the error, specifically on the training data. This distinction gives SVM a better baseline for generalization, which is crucial for statistical learning. SVR is a computational technique that extends the capabilities of SVM to address regression and prediction tasks. One of the key features of SVR is its objective to minimize the training error noticed throughout the learning process. Additionally, SVR aims to minimize the generalized error bound to get performance that is applicable beyond the training data. In regression tasks involving SVM, the SVR must employ a cost function C to quantify the empirical risk and then reduce the regression error. Additionally, epsilon insensitive loss  $\varepsilon$  controls the smoothness, complexity, and accuracy of the approximation function of SVR. Greater C and  $\varepsilon$  are more complex learning of SVM and *vice versa* [64]. Figure 5 shows the schematic view of the SVR algorithm. The SVR problem can be formalized using the following equation:

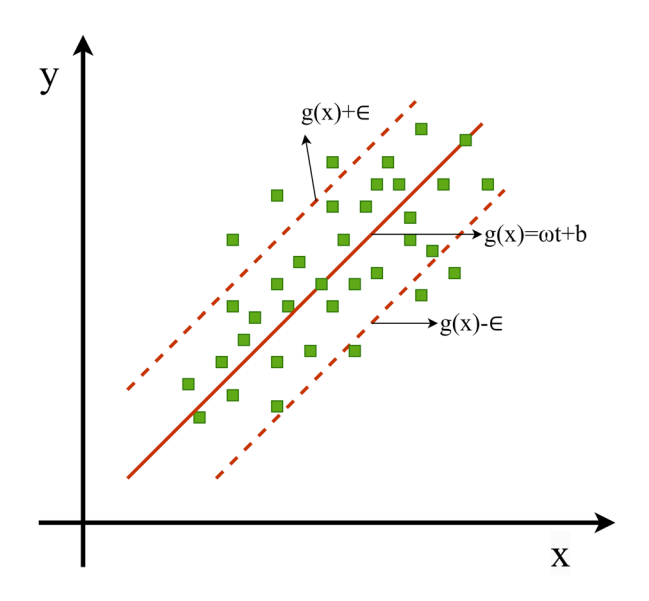


Figure 5: Schematic view of SVR.

$$\min \frac{1}{2} ||\omega||^2 + c \sum_{i=1}^m L(t_i, g(x_i)), \tag{1}$$

$$\begin{cases} \frac{1}{2} ||\omega||^2 + c \sum_{i=1}^m L(t_i, g(x_i)) \\ s.t. \begin{cases} t_i - g(x_i) \le \delta + \zeta_i^+ \\ g(x_i) - t_i \le \delta + \zeta_i^- \end{cases} \end{cases}$$
(2)

where  $\omega$  is a vector, which determines the slope of the fitted line; C is the regularization coefficient;  $L(t_i, g(x_i))$  is the insensitive loss function;  $\zeta + i$ ,  $\zeta - i$  (i 1, 2, ..., n) relaxation variable;  $\delta$  is the coefficient related to the interval band;  $g(x_i)$  is a fitted value; and  $t_i$  is a sample true value.

#### 2.2.3 GBR

The GBR model was introduced by Friedman in 1999 as an ensemble technique for regression and classification. The training set is chosen randomly, and the gradient boosting approach compares each iteration to the base model. Regression happens faster when the training data percentage is lower, while the GBR model fits smaller data in each iteration. The GBR model's tuning parameters include n trees and the shrinkage rate. n trees are the number of

trees that must be created, whereas the shrinkage rate is commonly known as the learning rate that is applied to each tree throughout the expansion process [65].

The core principle of this algorithm is based on the concept of boosting. The boosting procedure facilitates the transformation of predictions from a "weak" learner throughout the process of additive training. One of the main advantages of GBR algorithms is their ability to mitigate overfitting and optimize computing resources by utilizing an objective function. In addition to enhancing output performance, GBR methods also effectively minimize the specified error function, as stated in a previous study [66].

#### 2.2.4 GEP

The GEP is a branch of GP that was developed by Ferreira [67]. A function set, a terminal set, a fitness function, a set of control parameters, and a terminal condition are the fundamental components of GEP. The first three parts control the search space for the algorithm, while the latter two deal with search speed and quality. Due to GEP's multigenic architecture, it is possible to build nonlinear, multi-part programs. GEP's primary functionality is the generation of chromosomes through the use of the Karva

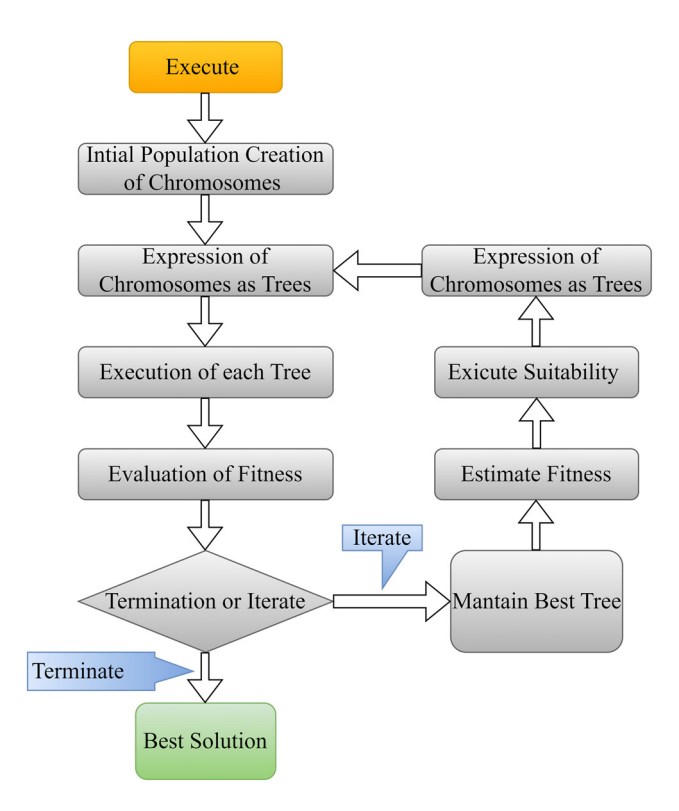


Figure 6: Schematic view of GEP.

language to express any parse tree capable of decoding and expressing the chromosome's stored data. Thus, chromosomes convert to expression tree branch structures. Karva expression (KE) transformation to expression tree (ET) begins at the initial position and extends through the string. String generation utilizes the inverse translation of ET to KE and a record of nodes from the root to the deeper layer [68]. Numerous solutions are initially created, and their fitness is determined using the basic GEP algorithm. The most appropriate chromosomes undergo operator modification before being passed on to the next generation. The problem's answer is then illustrated by eTs. By reading ET from top to bottom and then from left to right, it is possible to acquire the mathematical formula [69]. Figure 6 illustrates the sequential stages of the GEP algorithm. The process commences by generating chromosomes of a certain length for each individual in a random manner. The fitness of every individual is evaluated after the chromosomes are expressed as eTs. Only the most suitable individuals are selected for the reproductive process. The iteration incorporates individuals from several generations until an optimal solution is achieved. Genetic operations, including mutation, crossover, and reproduction, are employed to influence the population [70].

#### 2.2.5 Stacking ensemble

The stacking approach integrates the results from many learners utilizing a multilayer learning structure [71]. Base learners denote the first layer of a two-layer learning architecture, and meta-learners denote the second layer. The primary principle of the stacking model includes initial data training of the base learners. This ultimately generates a new set of data from each base learner output, which is subsequently trained on this new dataset to develop a final prediction model employing the meta-learner second layer.

In other words, the ensemble stacking algorithm produces the training dataset, utilizing the base learner as a training set for the meta-learner. The meta-learn model might be susceptible to overfitting in such a case where the base learner training is done as the new training set [72]. The framework of stacking is illustrated in Figure 7.

#### 2.2.6 Shapley adaptive exPlanations (SHAP)

The feature relevance of tree-based ensemble learning methods like RF is intrinsic [73]. This importance can be found by counting the number of times a characteristic appears when building the model tree. Analyzing feature importance scores in distinct ways, however, does not provide a comprehensive understanding of the overall impact of features or the positive and negative correlations between features and the corresponding output. Therefore, it is crucial to ascertain the overall importance of features inside the model and their connections to its aims. This is accomplished by SHAP analysis, as recommended by Lundberg and Lee [74]. The SHAP analytical approach is based on principles from game theory. The components of this analysis are treated as agents that influence the goal variables. The analysis provides a comprehensive overview of the gaming engagement of each participant [74]. The outcome is determined by the SHAP analysis process using Shapley values, which are based on well-established models. Global feature relevance in SHAP analysis is calculated by taking the average of the Shapley values for all features in the dataset. The values are presented on a plot after being organized in descending order. Each data point on the figure represents the Shapley value attributed to a particular feature and instance. The Shapley values are represented on the x-axis, while the feature importance is represented on the y-axis. The vertical position on the y-axis corresponds to the influence of the attributes on the target variable, while the color gradient

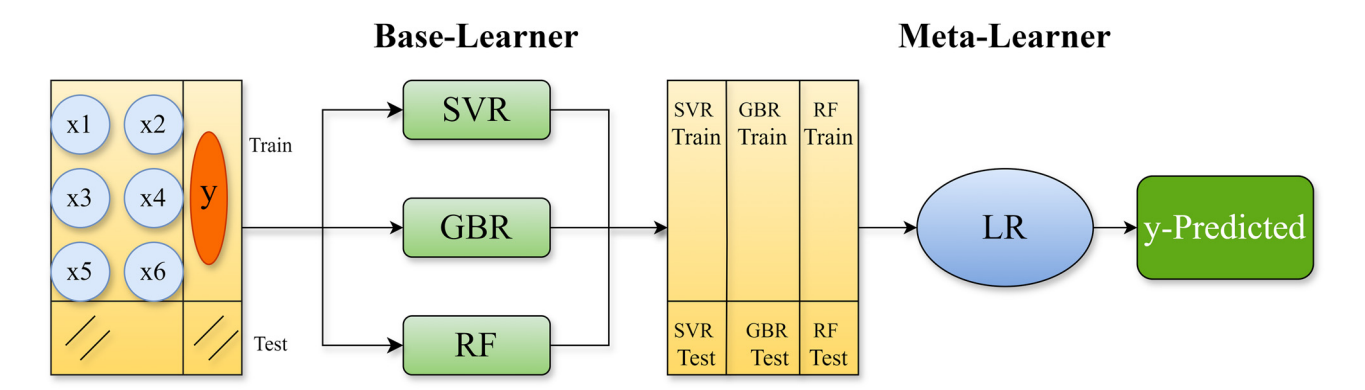


Figure 7: Framework of stacking ensemble.

reflects their level of importance. Moreover, SHAP-feature dependence plots clearly illustrate the impact of feature interactions on the target variable using color-coded representations. This approach provides a more extensive range of information compared to traditional partial dependence charts. Additional details regarding the SHAP plots [73].

Lundberg and Lee [74] proposed multiple versions of the SHAP analysis, including DeepSHAP, LinearSHAP, Kernel SHAP, and TreeSHAP. This study employed Tree-SHAP, a method that utilizes a linear explanatory model and Shapley values [28]. The initial prediction model has been formulated as

$$j(r') = \varnothing o + \sum_{q=1}^{n} \varnothing q r' q,$$
 (3)

where j, r', and N denote the explanation model, basic features, and maximum size of the collection, respectively. The symbol  $\varnothing$  is used to represent feature attribution. The estimation of the attribution of each attribute is performed using the following equations [74]:

$$\emptyset q = \sum_{H \subseteq Z\{q\}} \frac{|H|!(M|H|1)!}{M!} [kc(H \cup \{q\})kc(H)], \quad (4)$$

$$kc(H) = E[k(c)|cH], (5)$$

where H, Z, and E[k(c)|cH] indicate a subset of features, the entire set of inputs, and the desired result of the function on subset S, respectively.

# 2.3 Model development and performance evaluation

#### 2.3.1 Stacking model development

Before developing the prediction model, it is important to determine the best data split so that the model has a higher generalization capability. Since the established database differs in size, numerous data splits, such as the ratio of 70:30, 75:25, and 80:20 for model training and testing, were investigated in this study. Finally, the dataset was randomly split into training and testing sets for SPT and FS at 80, 20, 70, and 30%, respectively. The precision of the model is significantly influenced by the hyperparameters. Through optimization, the ML model's performance can be improved by identifying the hyperparameters that work best on the dataset. The grid search technique was utilized to optimize the hyperparameters of the ML model. The grid search method is a methodical strategy that entails extensively exploring a range of hyperparameter variations and training the model numerous times. The configuration

that yields the best outcomes throughout several training sessions is referred to as the ideal combination of hyperparameters.

The most effective hyperparameter combinations for predicting SPT in RHAC are as follows: RF model parameters: n estimators = 80, min samples leaf = 2, max depth = 10, min samples split = 3, and max features = 5. In the SVR model, the most effective combination of hyperparameters is degree = 3, gamma = 0.1, C = 10.0, epsilon = 0.3, and tol = 0.001. In the GBR model, the most effective hyperparameter combination is max depth = 3, learning rate = 0.02, and n estimators = 100.

Similarly, for the FS prediction models, the most effective hyperparameter combination in the RF model is n estimators = 100, min samples leaf = 2, min samples split = 4, and max features = 8. In the SVR model, the most effective combination of hyperparameters is degree = 3, gamma = 0.05, C = 20.0, epsilon = 0.15, and tol = 0.001. In the GBR model, the most effective hyperparameter combination is max depth = 3, learning rate = 0.05, and n estimators = 100.

#### 2.3.2 GEP model development

The SPT and FS of RHAC were considered to be functions of the following parameters:

SPT, TS = 
$$f(RHA, C, SP, Age, CA)$$
. (6)

The GEP models were developed in GeneXproTools 5.0. The parameters, such as population size, were deduced based on a trial-and-error approach. The program's execution time is determined by the population size, which refers to the number of chromosomes. The population size evaluated for the prediction models was either 50, 100, or 150, considering their number and complexity. The design of various models in the program is contingent upon the size of the head and the number of genes, with the former deciding the intricacy of each component and the latter dictating the number of sub-ETs in the model. In this study, the number of genes was set to 6 for both SPT and TS and two different head sizes: 6 and 8. The linkage functions for both models are multiplications, and the function sets considered for the models are addition, multiplication, subtraction, division, power, square root, and trigonometric functions. The precise parameters employed in the GEP method for both models are given in Table 3.

Several statistical metrics, including root mean square error (RMSE), relative root mean square error (RRMSE), mean absolute error (MAE), and correlation coefficient (R), were used to evaluate the performance of the developed

Table 3: Hyperparameters of the GEP model for SPT and FS

	GEP	
Hyperparameters	Tuned value for SPT	Tuned value for FS
Linkage function	Multiplication	Multiplication
Chromosomes	150	125
Head size	6	8
Genes	6	6
Tail size	7	9
Gene size	20	26
Dc size	7	9

models. The range of values for R is bounded between 0 and 1, where a higher R-value indicates a superior model. Conversely, when the values of RMSE, MAE, and RRMSE are lower, it suggests that the model exhibits better performance. Furthermore, the researchers also estimated a performance index  $(\rho)$  [75],

which served as a composite measure of the model's effectiveness by incorporating both the RRMSE and R. The variable  $\rho$  assumes values within the range of zero to positive infinity, with a lower value indicating a higher level of model performance. Eqs. (7)–(11) representing these metrics are as follows:

RMSE = 
$$\sqrt{\frac{\sum_{i=0}^{n} (ye_i - yp_i)^2}{n}}$$
, (7)

RRMSE = 
$$\frac{1}{|\overline{ye}_i|} \sqrt{\frac{\sum_{i=0}^{n} (ye_i - yp_i)^2}{n}},$$
 (8)

$$MAE = \frac{\sum_{i=0}^{n} |ye_i - yp_i|}{n},$$
(9)

$$R = \frac{\sum_{i=1}^{n} (y \mathbf{e}_{i} - \overline{y} \overline{\mathbf{p}}_{i})(y \mathbf{p}_{i} - \overline{y} \overline{\mathbf{p}}_{i})}{\sqrt{\sum_{i=1}^{n} (y \mathbf{e}_{i} - \overline{y} \overline{\mathbf{p}}_{i})^{2} \sum_{i=1}^{n} (y \mathbf{p}_{i} - \overline{y} \overline{\mathbf{p}}_{i})^{2}}},$$
 (10)

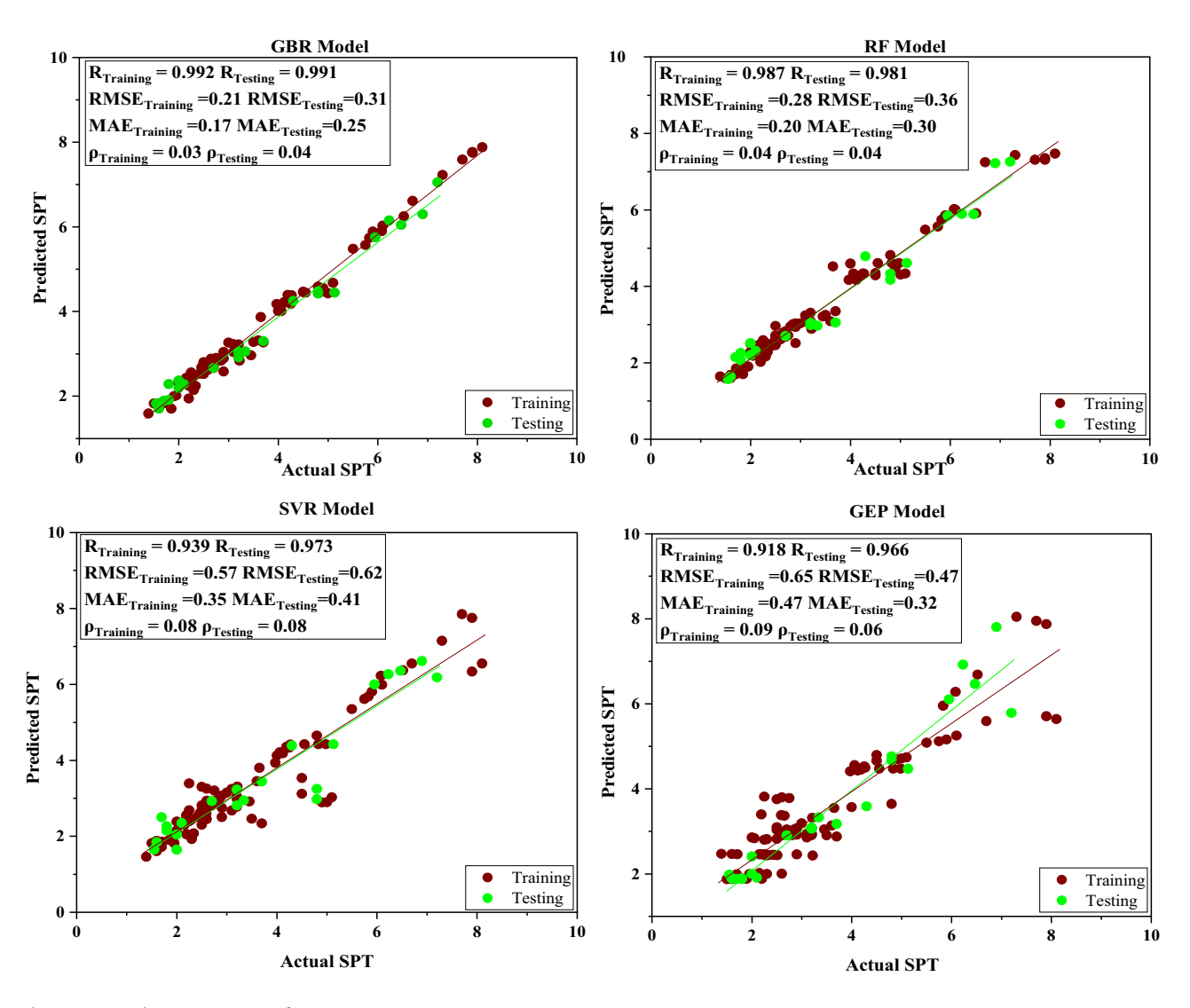


Figure 8: Base-learner outcomes for SPT.

$$\rho = \frac{\text{RRMSE}}{1+R},\tag{11}$$

where  $ye_i$  is the experimental value,  $yp_i$  is the predicted value associated with each of the parameters,  $\overline{ye}_i$  is the average experimental value,  $\overline{yp}_i$  is the average predicted value, and n is the total quantity of data.

# 3 Results and discussion

# 3.1 Base-learner and GEP prediction outcomes for SPT

In Figure 8, the experimental and predicted values for SPT for all models are shown juxtaposed with the absolute

error and statistical metrics such RMSE, MAE, etc. Figure 8 illustrates the efficacy of the models in precisely predicting the SPT of RHAC. Determining the GBR, RF, SVR, and GEP models' robustness was executed by analyzing their prediction outcomes and associated errors. During the training phase, the GBR, RF, SVR, and GEP models obtained R values of 0.992, 0.987, 0.939, and 0.918, respectively. During the testing phase, the recorded values were 0.991, 0.981, 0.973, and 0.966, respectively. These results indicate a significant relationship between the experimental and predicted outcomes. The RMSE values for the models during the training phase were 0.21, 0.28, 0.57, and 0.65, respectively. Similarly, during the testing phase, the RMSE values were 0.31, 0.36, 0.62, and 0.47. During the training phase, the MAE values were recorded as 0.17, 0.20, 0.35, and 0.47. In the subsequent testing phase, the

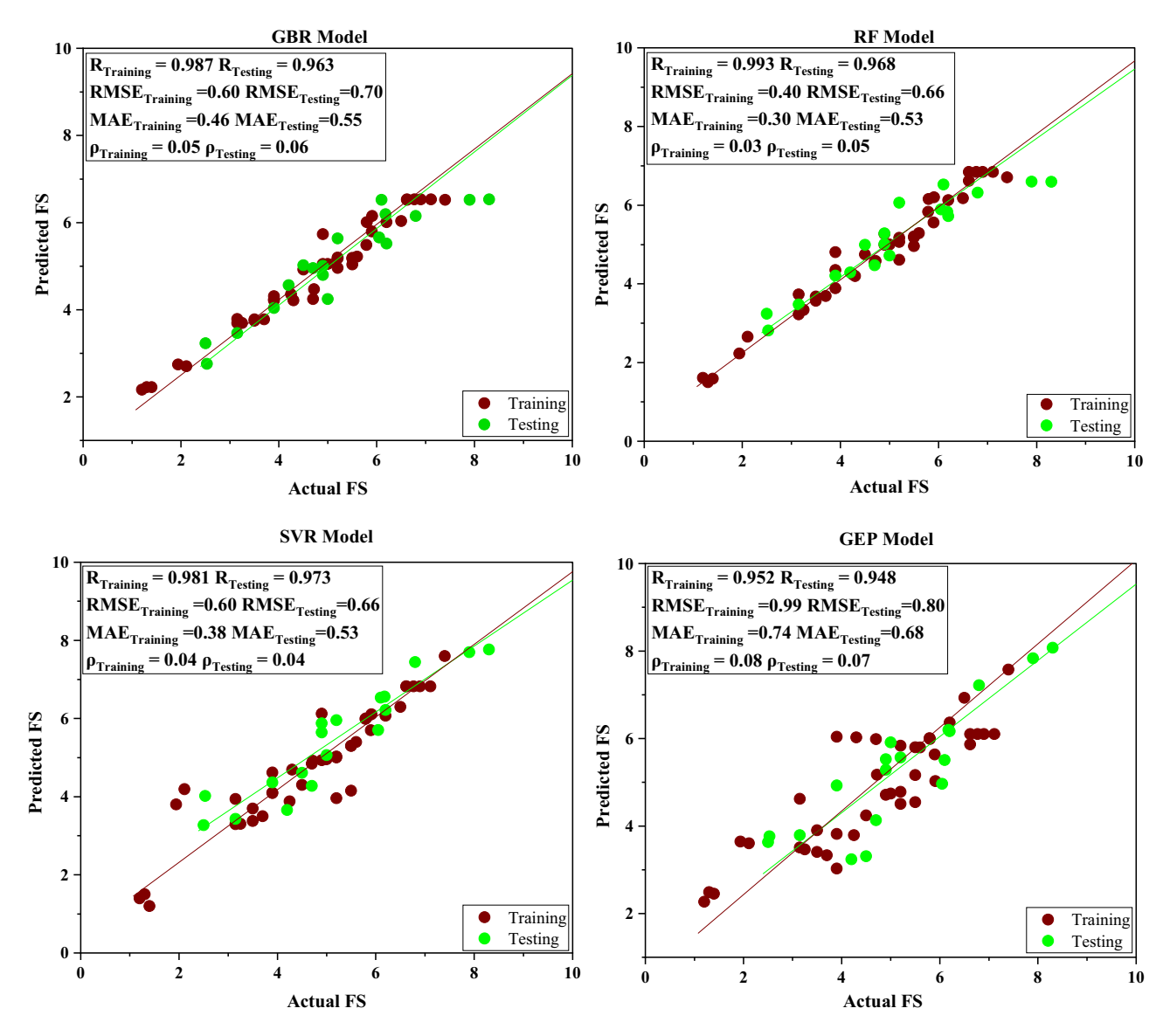


Figure 9: Base-learner outcomes for FS.

MAE values were observed to be 0.25, 0.30, 0.41, and 0.32. The statistics consistently exhibited little variance throughout all datasets.

# 3.2 Base-learner and GEP prediction outcomes for FS

The predicted and experimental results for FS can be seen in Figure 9. The performance of each ML model is gauged by the values of statistical indicators, as previously discussed. For both the training and testing phases, the GBR, RF, SVR, and GEP models exhibited high *R* values. Specifically during the training phase, the *R*-values were 0.987, 0.993, 0.981, and 0.952, respectively, while in the testing phase, they were 0.963, 0.968, 0.973, and 0.948. This demonstrates a strong correlation between the actual and predicted values. In the

training phase, the RMSE values for these models were 0.60, 0.40, 0.60, and 0.99, respectively, and the MAE values were 0.46, 0.30, 0.38, and 0.74. For the testing phase, the RMSE values were 0.70, 0.66, 0.66, and 0.80, and the MAE values were 0.55, 0.53, 0.53, and 0.68. All these details are visually represented in Figure 9.

# 3.3 Stacking prediction outcomes for SPT and FS

RF and SVR models for SPT and RF and GBR models for FS were chosen as the base learners of the stacking model, while the LR model was used as the meta-learner. The predicted results of the stacking model for SPT on the testing and training set are as follows: RMSE = 0.21, 0.30, MAE = 0.16, 0.23, and R = 0.991, 0.988, respectively, can be

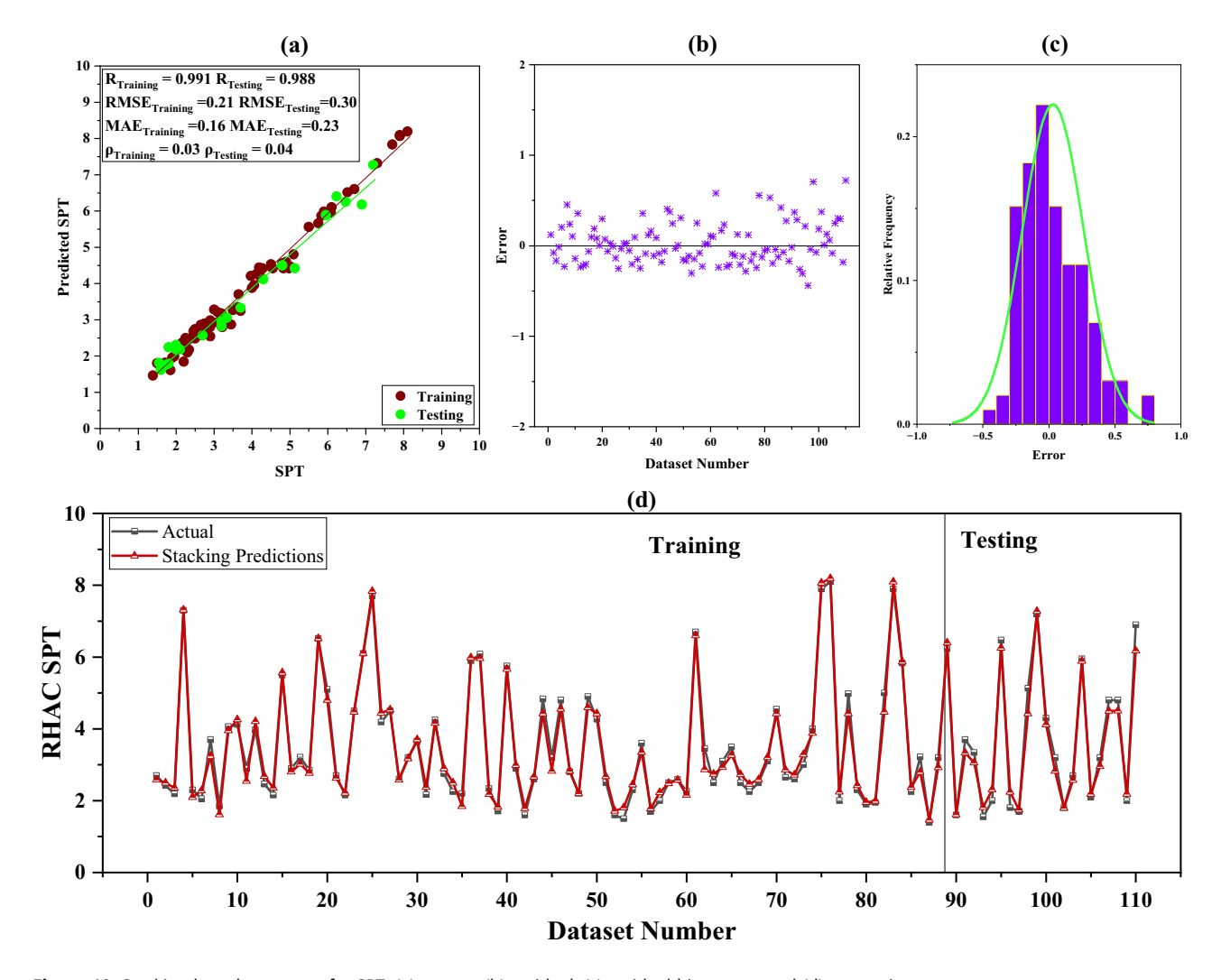


Figure 10: Stacking-based outcomes for SPT: (a) scatter, (b) residual, (c) residual histogram, and (d) comparison.

seen in Figure 10. Similarly, Figure 11 illustrates the stacking models' outcomes for FS on the testing and training set as follows: RMSE = 0.48, 0.72, MAE = 0.34, 0.50, and R = 0.988, 0.964.

The relationship between the predicted and actual values of the stacking model for SPT and FS of RHAC is depicted in Figures 10 and 11. In addition, the residuals and residual histograms are depicted in the figures. The stacking model analysis revealed an error range of –0.5 to 0.5 and –1 to 1 for SPT and FS, respectively. The stacking model outperforms each basic learner evaluating metrics that are compared between each of the four base learner models (GBR, RF, SVR, and GEP). This shows that the meta-learner in the stacking model corrects the samples that the base learner inadvertent predicted and increases the model's prediction accuracy.

## 3.4 GEP expressions

The effectiveness of the GEP model was assessed by analyzing the outcomes and errors of the predictions. By decoding the results from GEP, an empirical expression for calculating the SPT and FS of RHAC is derived. These expressions encompass the effects of all the independent variables considered in this study. The SPT and FS decoded equations are presented as Eqs. (12) and (13), respectively.

SPT = 
$$(g_1 \times g_2 \times g_3 \times g_4 \times g_5 \times g_6)$$
, (12)

whereas

$$\begin{split} g_1 &= (\cos(-8.56) + ((-8.02/W)/(5.34 - \text{SP}))), \\ g_2 &= ((\text{TAN(FA}) + (\text{RHA} + C)) \times ((\text{RHA} + \text{SP}) + C)), \\ g_3 &= (((-8.56 \times \text{age}) + (W - \text{FA})) + \text{TAN((FA} \times -7.41))), \end{split}$$

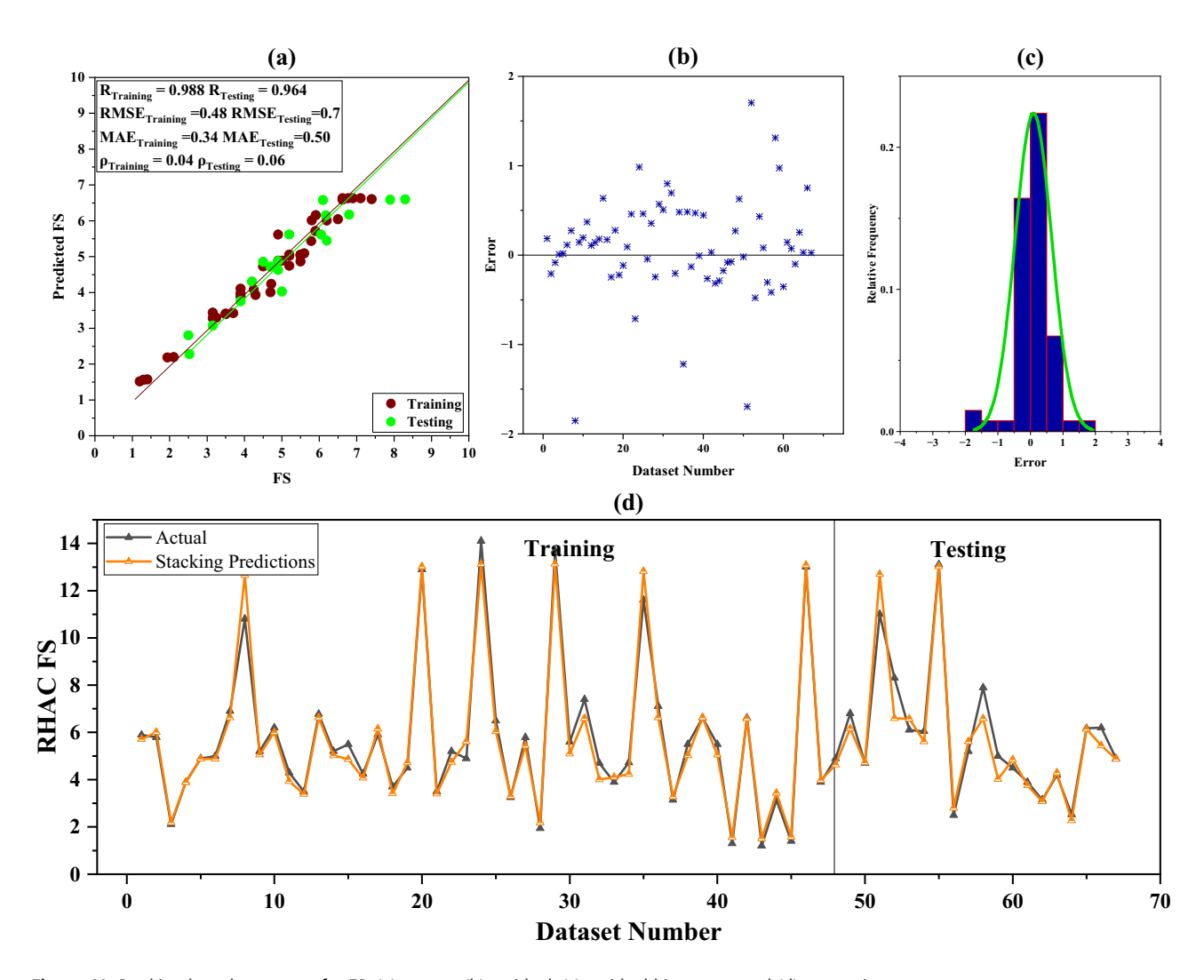


Figure 11: Stacking-based outcomes for FS: (a) scatter, (b) residual, (c) residual histogram, and (d) comparison.

$$g_4 = ((((-33.48 - 33.48) + FA)^{-2.99})/FA),$$

$$g_5 = (-11.95 \times (((-28.61 \times -28.61) - FA) + (21.12 - FA))),$$

$$g_6 = (((Age + SP + C) + (SP^{2.15}))/C),$$

$$FS = (G_1 \times G_2 \times G_3 \times G_4 \times G_5 \times G_6),$$
(13)

whereas

$$G_{1} = (2 \times 20.97 + (((RHA - W) \times (-3.95)) + (FA \times (-2.41)))),$$

$$G_{2} = (FA/(TAN(TAN(FA)) - POWER((FA + C), (5.921 + (-1.63))))),$$

$$G_{3} = ((Age + SP) - (-13.21 - TAN((-6.39 \times FA)))),$$

$$G_{4} = (SQRT(FA) \times (((-15.29 \times SP) - (-15.29 + (-7.13))) - (C - A))),$$

$$G_{5} = \frac{(C - ((SIN(FA) - 1.531) \times (-2 \times 32.04)))}{FA},$$

 $G_6 = ((((RHA \times SP) + (8.84 \times W))/(SIN(W) - Age)) - C).$ 

## 3.5 SHAP analysis

The SHAP value analysis for the models is depicted in Figure 12(a) and (b). The beeswarm plot in SHAP analysis displays color codes and the importance of feature values on the right side. The SHAP analysis, depicted in a beeswarm plot, demonstrates that the results obtained from the RF model are consistent with the experiment results. Figure 12(a) and (b) demonstrates that the W, C, and age and W, SP, and age significantly impact the SPT and FS model's output, respectively. Lower W and higher C, SP, and age have shown a positive impact on the model output (i.e., SPT and FS)

The SHAP dependence plots for SPT are shown in Figure 13(a)-(f). Figure 13(a) illustrates the SHAP dependence plot for C and W, showing their direct interaction. The strength tends to decrease when both C and W are high. However, an optimal W combined with a high C results in a positive SHAP value (SPT). Figure 13(b) depicts the W and C, revealing a direct interaction. Elevated values of both W and C reduce the SHAP value. Figure 13(c)

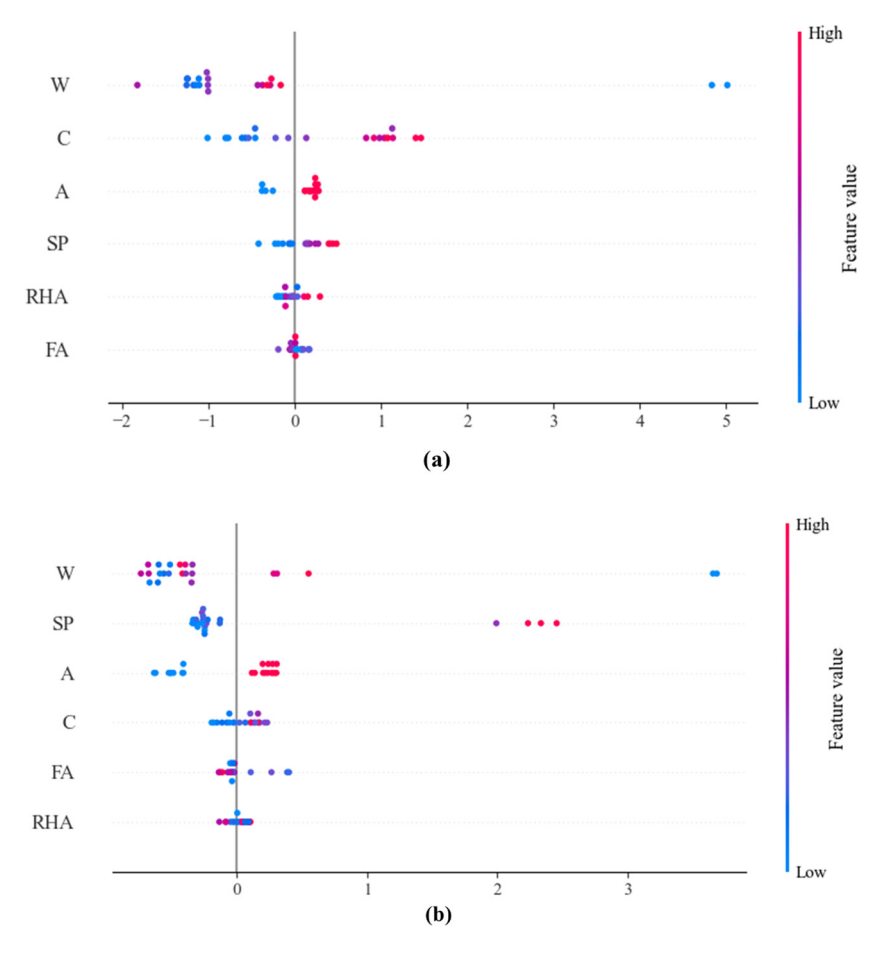


Figure 12: SHAP analysis beeswarm plot for (a) SPT and (b) FS.

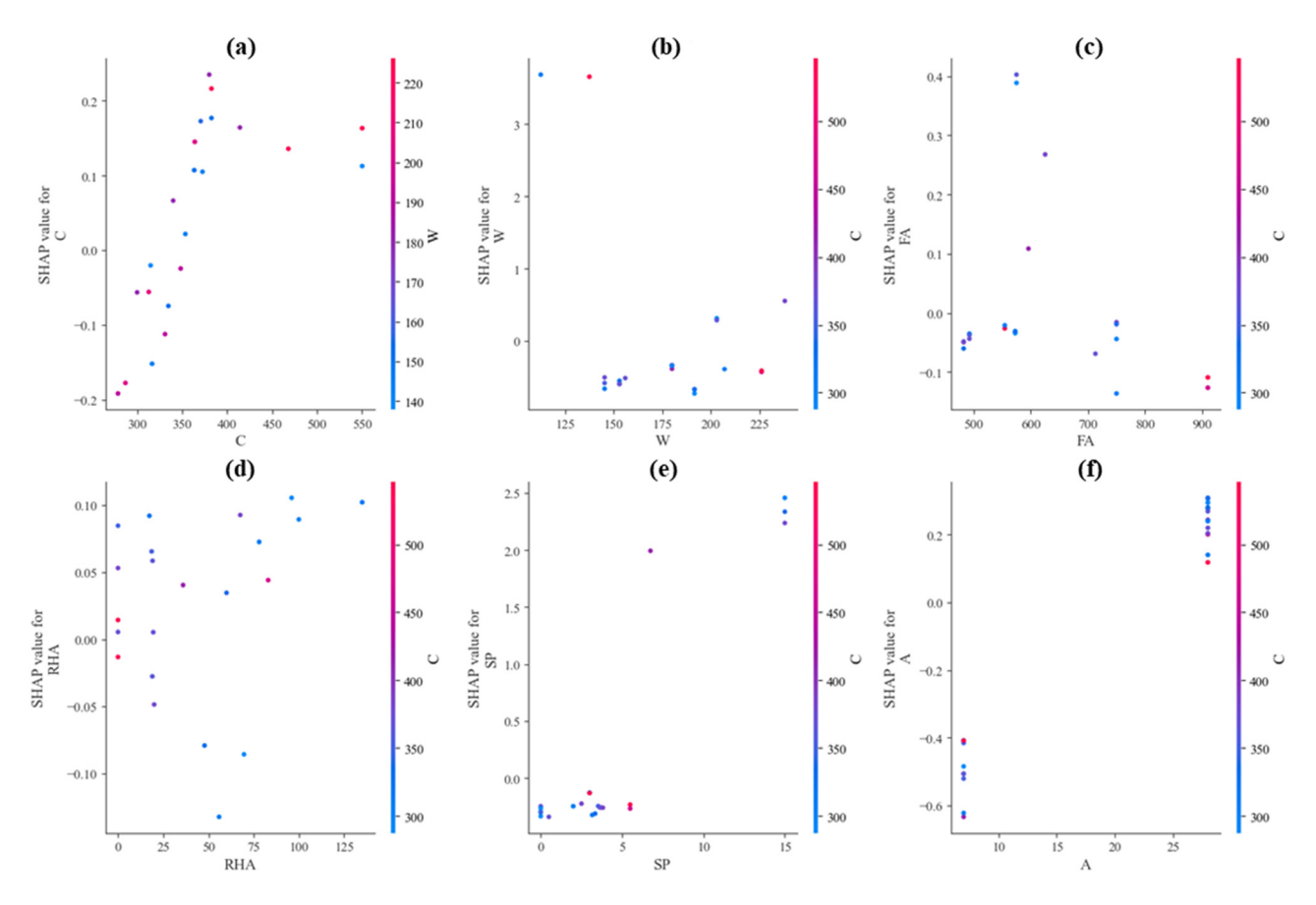


Figure 13: Feature dependency of the model for SPT. (a) C, (b) W, (c) FA, (d) RHA, (e) SP, and (f) A.

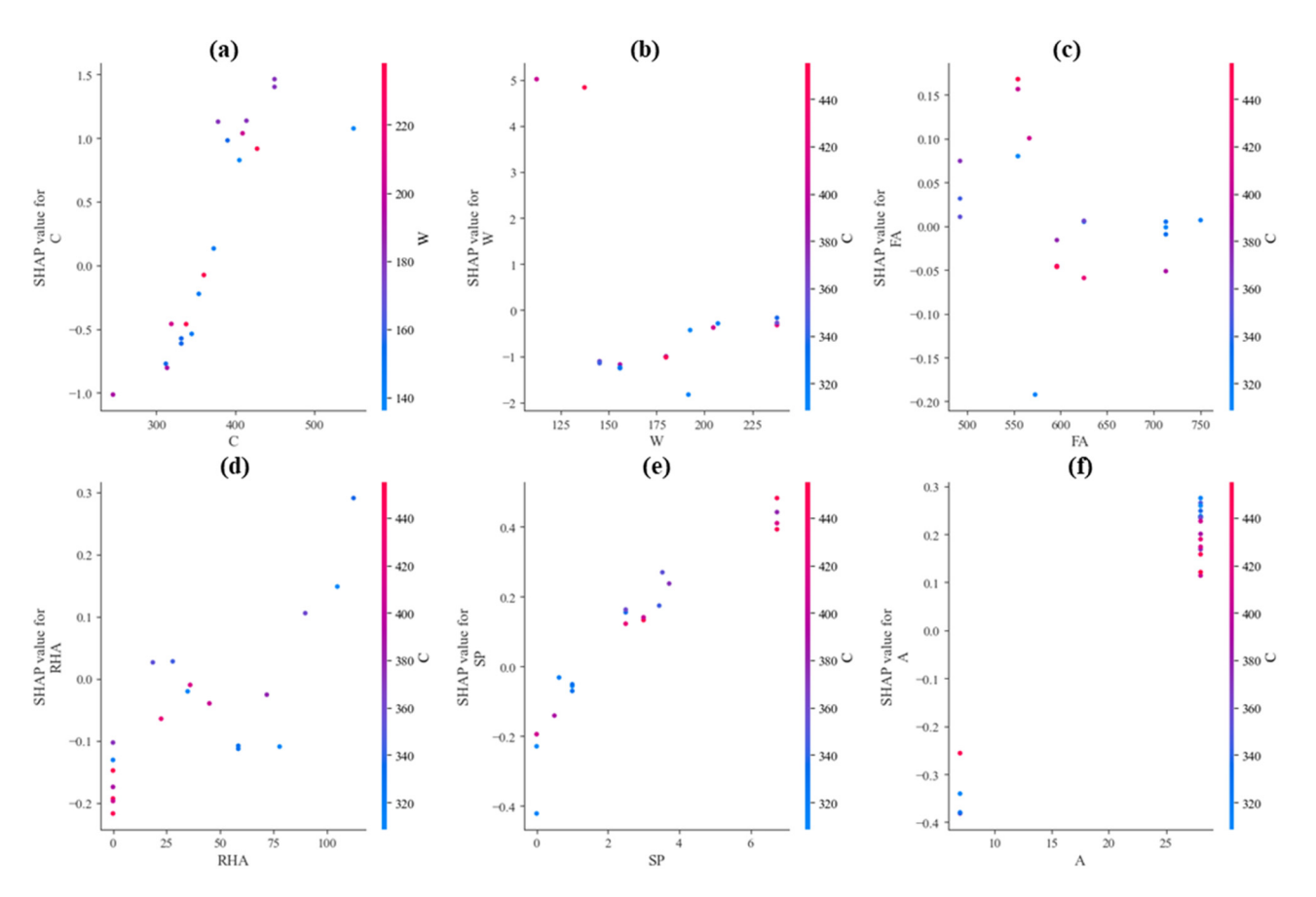


Figure 14: Feature dependency of the model for FS. (a) C, (b) W, (c) FA, (d) RHA, (e) SP, and (f) A.

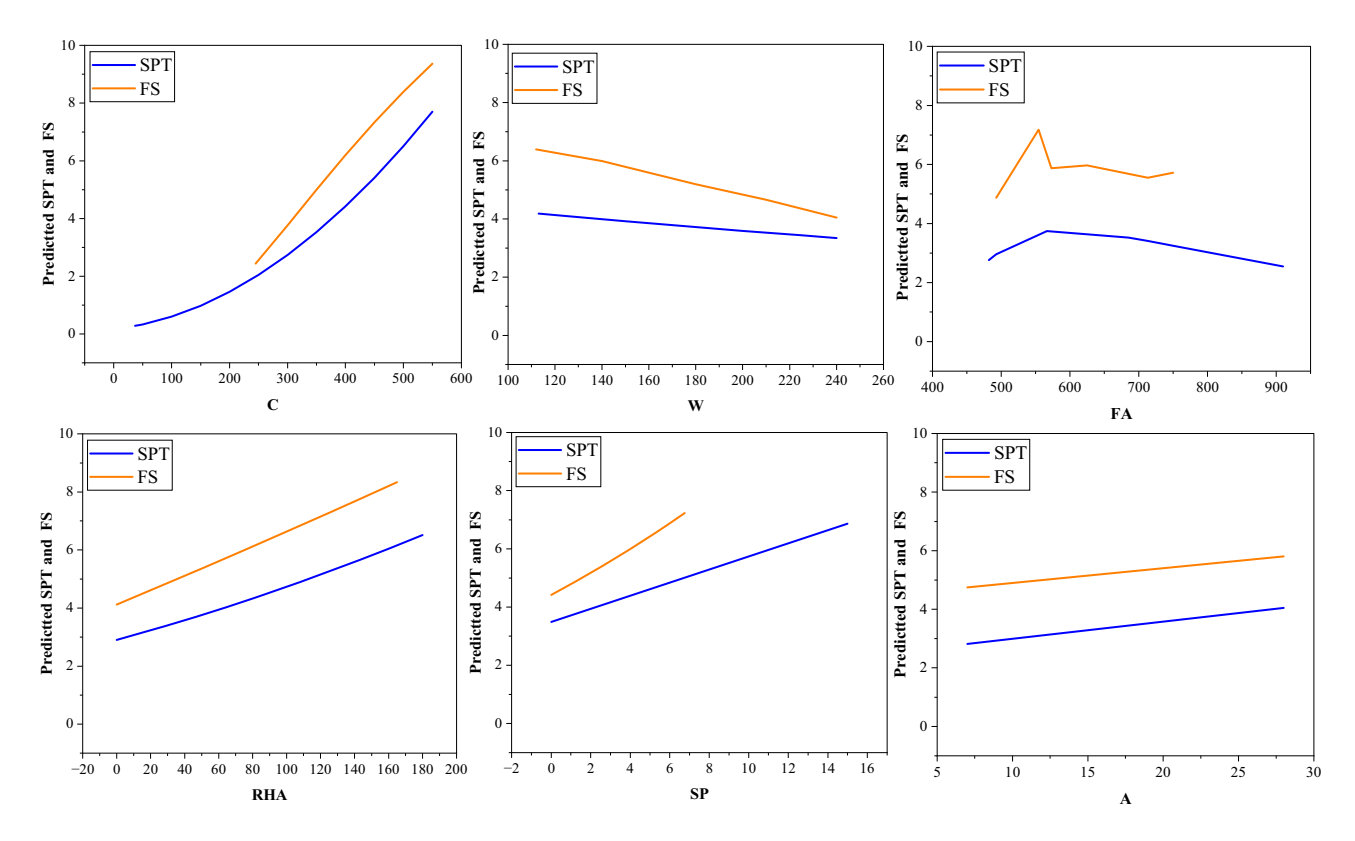


Figure 15: Parametric analysis for SPT and FS.

presents the interaction between FA and *C*. FA has a direct relationship with *C*. An increase in FA combined with an optimal *C* boosts the strength. Lower feature values of both RHA and FA diminish the strength, while their higher values enhance it, as depicted in Figure 13(d). Figure 13(e) depicts the interaction between SP and RHA. A direct relationship is evident, with an increase in both SP and RHA leading to greater strength. Figure 13(f) depicts the relationship between age and *W*. A higher age (*A*) combined with an optimal *W* increases strength.

Figure 14(a)–(f) display the SHAP dependence plot for FS. Figure 14(a) depicts the SHAP dependence plots for the  $\cal C$ 

and W features, revealing an inverse interaction between them. Specifically, when C is high and W is low, the SHAP value (TS) decreases. However, the SHAP value turns positive with an optimal and a higher C. Figure 14(b) depicts the features W and C, indicating an inverse interaction. A combination of lower W and higher C results in increased strength. Figure 14(c) depicts diagrams for features FA and C. FA directly interacts with C. An increase in FA combined with an optimal C boosts strength, while higher FA and lower C diminish it. Figure 14(d)–(f) depict the direct interactions of RHA, SP, and age with C, respectively. In each case, higher RHA, SP, and age, when combined with a greater C, enhance the strength.

Table 4: Performance evaluation of base learners

			Trai	ning		Testing				
	Model	MAE	RMSE	R	ρ	MAE	RMSE	R	ρ	
SPT	GBR	0.17	0.21	0.992	0.03	0.25	0.31	0.991	0.04	
	RF	0.20	0.28	0.987	0.04	0.30	0.36	0.981	0.04	
	SVR	0.35	0.57	0.939	0.08	0.41	0.62	0.947	0.08	
	GEP	0.47	0.65	0.919	0.09	0.32	0.47	0.966	0.06	
FS	GBR	0.46	0.60	0.987	0.05	0.55	0.70	0.963	0.06	
	RF	0.30	0.40	0.993	0.03	0.53	0.66	0.968	0.05	
	SVR	0.38	0.60	0.981	0.04	0.53	0.66	0.973	0.04	
	GEP	0.74	0.99	0.952	0.08	0.68	0.80	0.948	0.07	

Table 5: Performance evaluation of stacking

			Trai	ning			Tes	ting	
	Model	MAE	RMSE	R	ρ	MAE	RMSE	R	ρ
SPT	Stacking	0.16	0.21	0.992	0.03	0.23	0.30	0.988	0.04
FS	Stacking	0.34	0.48	0.988	0.04	0.50	0.7	0.965	0.06

#### 3.6 Parametric analysis

This study performs a parametric analysis in addition to depending on historical patterns to acquire a deeper knowledge of the mechanical properties of RHAC. This analysis aims to verify the GEP expressions and assess the influence of particular input features on the mechanical properties while maintaining other variables constant. To observe the impact on the SPT and FS, one input variable was changed from its minimum to maximum value. The results of a parametric analysis using the constructed GEP models are displayed in Figure 15. It was determined that there is a positive correlation between an increase in *C*, RHA, SP, and age and an increase in SPT and FS of RHAC. Additionally, it was observed that an increase in *W* results in a significant decrease in strength. The results of the parametric analysis are consistent with the experimental investigation and reinforce the interpretations of previous studies [76].

Tables 4 and 5, Figure 16 demonstrate that all models' R values for both the training and testing datasets exceed 0.9. Additionally, the MAE and RMSE values for the stacking models are better than base learners and lower than 0.75 MPA. The  $\rho$  values of the training and testing datasets for all the models approach zero. Hence, it has been discovered that all the models are acceptable and can be utilized to predict the SPT and FS of RHA concrete. Furthermore, comparing the matrices results of the base learners, stacking, and GEP demonstrated that stacking outperforms GEP for both SPT and TS of RHAC. In addition, the FS stacking results are comparable to the SVR model. Moreover, considering the validation of the GEP expression using parametric analysis, the expressions are applicable and recommended for the routine design of RHAC SPT and FS.

used various statistical metrics, such as MAE, RMSE, and R.

# 4 Models' performances evaluation

The study used an extensive evaluation strategy to evaluate the effectiveness of the developed models. The evaluation

#### 4.1 External validation conditions

Golbraikh and Tropsha [77] and Roy and Roy [78] both recommended an external validation criterion to evaluate the generalization of the models. Numerous research

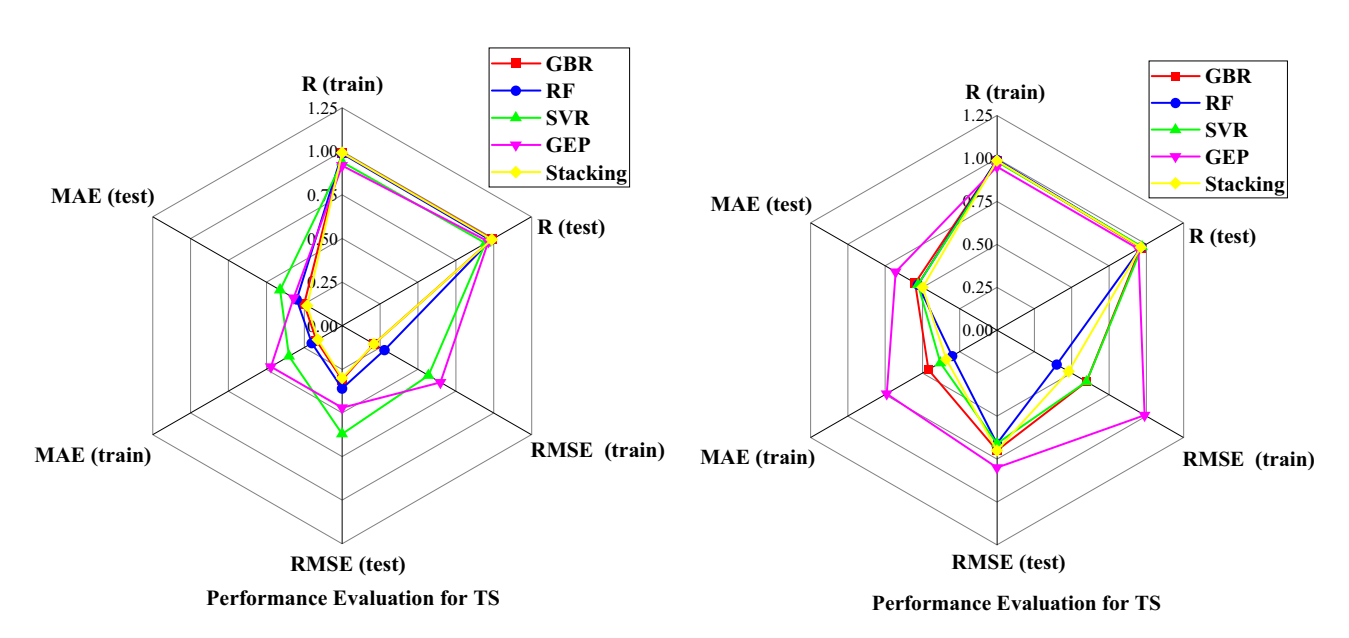


Figure 16: Radar graph for model's performance evaluation for SPT and FS.

 Fable 6:
 External validation conditions of proposed models

S.No.	Equations	Condition			SPT					FS		
			Stacking	GBR	RF	SVR	GEP	Stacking	GBR	RF	SVR	GEP
_	$k = \frac{\sum_{i=0}^{n} (ye_i \times yp_i)}{ve_i^2}$	0.85 < <i>k</i> < 1.15	0.994	1.009	1.019	0.994	0.994	0.972	1.006	0.972	1.040	1.047
2	$k' = \frac{\sum_{i=0}^{l} (y e_i \times y p_i)}{v r_i^2}$	0.85 < <i>k'</i> < 1.15	1.014	1.000	0.994	1.041	1.014	1.038	1.007	1.038	0.987	986.0
m	$m = \frac{R^2 - R_0^2}{R^2}$	<i>m</i> < 0.1	-0.019	- 0 003	0.011	-0.113	-0.067	-0.026	- 0.073	- 0.026	0.068	0.049
4	$n = \frac{R^2 - R_0'^2}{R^2}$	<i>n</i> < 0.1	0.010	-0.017	- 0.035	- 0.024	- 0.035	0.041	-0.071	0.041	- 0047	1 0
2	$R_0^2 = 1 - rac{\sum_{l=1}^{l} (y p_l - y e_l^0 \gamma^2)}{\sum_{l=1}^{l} (y p_l - y p_l^0 \gamma^2)}, y e_l^0 = K  imes y e_1$	$R_0^2 \approx 1$	966.0	986.0	0.951	0.999	0.996	0.955	966.0	0.955	0.880	0.854
9	$R_0'^2 = 1 - \left[ \frac{\sum_{i=1}^n (y e_i - y p_i^0)^2}{\sum_{j=1}^n (y e_i - y p_j^0)^2} \right], y p_i^0 = K' \times y e_i$	$R_0^{\prime 2} \approx 1$	996.0	666.0	966.0	0.929	0.966	0.892	0.995	0.892	0.990	0.990
7	$R_m = R^2 (1 - \sqrt{ R^2 - R_0^2 })$	$R_m > 0.5$	0.840	0.922	0.862	0.611	0.699	0.783	0.686	0.783	0.704	0.708

papers [28,31,64,79] have endorsed this method. The external validation criteria and the equation to determine the model's robustness are given in Table 6. The stacking and all base learner models have met the external validation criteria. As evidenced in Table 6, k and k' are close to 1. In addition, the performance index values, especially m and n, register values below 0.1. Moreover,  $R_0^2$  and  $R_0'^2$  are either nearing 1 or, in some cases, approximately equal to the  $R^2$  of the respective models.

Therefore, the external evaluation results of the models not only meet the needed standards but also demonstrate an outstanding capacity to predict the SPT and FS. These models provide acceptable prediction insights by transcending more connections between independent and dependent variables.

# 5 Conclusion

This study developed a stacking ensemble learning-based RHAC SPT and FS prediction model to improve the prediction model's capabilities. Additionally, generalized expressions based on the GEP model were developed for RHAC's SPT and FS. The models were trained on a comprehensive dataset from the literature comprising 110 and 67 data points for SPT and TS, respectively. Experimental research was conducted to determine the superiority of the stacking ensemble approach and the rationalism of the chosen base learners in the stacking model. Eventually, the importance of the variables in the input was assessed using the SHAP analysis for the RF model and parametric analysis for the GEP models. The conclusions drawn from this study are as follows:

- For SPT and FS, the LR model was employed as the second-layer meta-learner, while the RF, SVR, and RF, GBR models were utilized as the first-layer base learners, respectively.
- 2) The established stacking model for SPT's performance evaluation indications for testing and training are as follows: RMSE = 0.21, 0.30, MAE = 0.16, 0.23, and R = 0.99, 0.988, respectively. Similarly, the values for FS are as follows: RMSE = 0.48, 0.72; MAE = 0.34, 0.50; and R = 0.988, 0.964. The stacking model effectively integrates the base learners' prediction results to enhance the model's predictive capability.
- 3) The GEP model has been trained effectively, showing a substantial correlation between the actual and predicted outcomes with low error values. For the model training, the RMSE, MAE, and *R* values of the SPT model were 0.65, 0.47, and 0.92, respectively, and the values

calculated for the testing were 0.47, 0.32, and 0.97. Similarly, for the FS model, the RMSE, MAE, and *R* values for the model training were 0.99, 0.0.74, and 0.95, respectively, while for the model testing, values were 0.80, 0.68, and 0.95. The GEP expression effectively incorporated the influence of input variables for predicting RHAC's SPT and FS. The parametric analysis validates the robustness of the model.

4) The SHAP analysis investigation for the RF reveals that *W*, *C*, *W*, SP, and age are the most influential variables that impact the SPT and FS of RHAC, respectively. Moreover, the parametric analysis of GEP models identified that *C*, RHA, SP, and age have a positive correlation, and *W* has a negative correlation for each respective strength attribute.

The developed ensemble-based learners, staking model, and GEP expressions apply specifically to the given range of datasets. The generalizations of the stacking and GEP models can be further enhanced by using a vast range of datasets and considering the age of RHAC. In addition, different expression techniques such as multi-GEP, hybrid genetic and simulated annealing, and neural network models could be developed to compare the results of stacking and the GEP models.

Acknowledgments: The authors acknowledge the facility's support with numerical calculations using the supercomputer located in the National Supercomputing Center in JiNan, Big Data Computing Center of Southeast University. This project was financially supported by the Natural Science Foundation of China (grant no. 51378104), the National Science Fund for Distinguished Young Scholars (grant no. 52125802), the "One belt, one road" innovation cooperation project under the policy guidance plan of Jiangsu Province (grant no. BZ2021011), and the Fundamental Research Funds for the Central Universities (2242022k30030, 2242022k30031). The authors extend their appreciation to the Deanship of Research and Graduate Studies at King Khalid University for funding this work through Large Research Project under grant number RGP2/176/45.

**Funding information:** This project was financially supported by the Natural Science Foundation of China (grant no. 51378104), the National Science Fund for Distinguished Young Scholars (grant no. 52125802), the "One belt, one road" innovation cooperation project under the policy guidance plan of Jiangsu Province (grant no. BZ2021011) and the Fundamental Research Funds for the Central Universities (2242022k30030, 2242022k30031).

Author contributions: Muhammad Waqas Ashraf: conceptualization, methodology, software, data curation, writing – original draft, visualization, investigation, software, validation, writing – review and editing. Adnan Khan: conceptualization, methodology, software, data curation, visualization, investigation, validation, writing – review and editing. Tu Yongming: methodology, visualization, investigation, supervision, validation, writing – review and editing. Wang Chao: visualization, investigation, supervision, validation, writing – review and editing. Nabil Ben Kahla: validation, writing – review and editing. Safi Ullah: software, data curation, Visualization. Jawad Tariq: software, data curation, visualization. All authors have accepted responsibility for the entire content of this manuscript and approved its submission.

**Conflict of interest:** The authors state no conflict of interest.

**Data availability statement:** The article contains citations to the dataset from where it is collected. In addition, the Excel macro files of the GEP models are available in the supplementary materials.

# References

- [1] Jaturapitakkul, C. and B. Roongreung. Cementing material from calcium carbide residue-rice husk ash. *Journal of Materials in Civil Engineering*, Vol. 15, 2003, pp. 470–475.
- [2] Rodríguez de Sensale, G. Strength development of concrete with ricehusk ash. Cement and Concrete Composites, Vol. 28, 2006, pp. 158–160.
- [3] Singh, B. Rice husk ash. Waste and Supplementary Cementitious Materials in Concrete, Woodhead Publishing, Elsevier, 2018, pp. 417–460.
- [4] Chopra, D. and R. Siddique. Strength, permeability and microstructure of self-compacting concrete containing rice husk ash. *Biosystems Engineering*, Vol. 130, 2015, pp. 72–80.
- [5] Kizhakkumodom Venkatanarayanan, H. and P. R. Rangaraju. Effect of grinding of low-carbon rice husk ash on the microstructure and performance properties of blended cement concrete. *Cement and Concrete Composites*, Vol. 55, 2015, pp. 348–363.
- [6] Zain, M. F. M., M. N. Islam, F. Mahmud, and M. Jamil. Production of rice husk ash for use in concrete as a supplementary cementitious material. *Construction and Building Materials*, Vol. 25, 2011, pp. 798–805.
- [7] Khan, M. N. N., M. Jamil, M. R. Karim, M. F. M. Zain, and A. B. M. A. Kaish. Filler effect of pozzolanic materials on the strength and microstructure development of mortar. *KSCE Journal of Civil Engineering*, Vol. 21, 2017, pp. 274–284.
- [8] Rukzon, S. and P. Chindaprasirt. Mathematical model of strength and porosity of ternary blend Portland rice husk ash and fly ash cement mortar. *Computers and Concrete*, Vol. 5, 2008, pp. 75–88.
- [9] Karthik, S., P. R. M. Rao, and P. O. Awoyera. Strength properties of bamboo and steel reinforced concrete containing manufactured

- sand and mineral admixtures. *Journal of King Saud University Engineering Sciences*, Vol. 29, 2017, pp. 400–406.
- [10] Singh, P. To study strength characteristics of concrete with rice husk ash. *Indian Journal of Science and Technology*, Vol. 9, 2016, pp. 1–5.
- [11] Bixapathi, G. and M. Saravanan. Strength and durability of concrete using Rice Husk ash as a partial replacement of cement. *Materials Today: Proceedings*, Vol. 52, 2022, pp. 1606–1610.
- [12] Paris, J. M., J. G. Roessler, C. C. Ferraro, H. D. DeFord, and T. G. Townsend. A review of waste products utilized as supplements to Portland cement in concrete. *Journal of Cleaner Production*, Vol. 121, 2016, pp. 1–18.
- [13] Hariharan, A. R. and A. S. Santhi. G. Mohan Ganesh, Statistical model to predict the mechanical properties of binary and ternary blended concrete using regression analysis. *International Journal of Civil Engineering*, Vol. 13, 2015, pp. 331–340.
- [14] Farooq, F., W. Ahmed, A. Akbar, F. Aslam, and R. Alyousef. Predictive modeling for sustainable high-performance concrete from industrial wastes: A comparison and optimization of models using ensemble learners. *Journal of Cleaner Production*, Vol. 292, 2021, id. 126032.
- [15] Datta, S. D., M. Islam, M.dH. Rahman Sobuz, S. Ahmed, and M. Kar. Artificial intelligence and machine learning applications in the project lifecycle of the construction industry: A comprehensive review. *Heliyon*, Vol. 10, 2024, id. e26888.
- [16] Jalal, F. E., M. Iqbal, W. A. Khan, A. Jamal, and K. Onyelowe. ANN-based swarm intelligence for predicting expansive soil swell pressure and compression strength. *Scientific Reports*, Vol. 14, 2024, id. 14597.
- [17] Awoyera, P. O., M. S. Kirgiz, A. Viloria, and D. Ovallos-Gazabon. Estimating strength properties of geopolymer self-compacting concrete using machine learning techniques. *Journal of Materials Research and Technology*, Vol. 9, 2020, pp. 9016–9028.
- [18] Bui, D.-K., T. Nguyen, J.-S. Chou, H. Nguyen-Xuan, and T. D. Ngo. A modified firefly algorithm-artificial neural network expert system for predicting compressive and tensile strength of high-performance concrete. *Construction and Building Materials*, Vol. 180, 2018, pp. 320–333.
- [19] Yan, K. and C. Shi. Prediction of elastic modulus of normal and high strength concrete by support vector machine. *Construction and Building Materials*, Vol. 24, 2010, pp. 1479–1485.
- [20] Nazari, A. and J. G. Sanjayan. Modelling of compressive strength of geopolymer paste, mortar and concrete by optimized support vector machine. *Ceramics International*, Vol. 41, 2015, pp. 12164–12177.
- [21] Altun, F., Ö. Kişi, and K. Aydin. Predicting the compressive strength of steel fiber added lightweight concrete using neural network. *Computational Materials Science*, Vol. 42, 2008, pp. 259–265.
- [22] Mohammed, A., L. Burhan, K. Ghafor, W. Sarwar, and W. Mahmood. Artificial neural network (ANN), M5P-tree, and regression analyses to predict the early age compression strength of concrete modified with DBC-21 and VK-98 polymers. *Neural Computing & Applications*, Vol. 33, 2021, pp. 7851–7873.
- [23] Ahmed, H. U., A. S. Mohammed, and A. A. Mohammed. Proposing several model techniques including ANN and M5P-tree to predict the compressive strength of geopolymer concretes incorporated with nano-silica. *Environmental Science and Pollution Research*, Vol. 29, 2022, pp. 71232–71256.
- [24] Emad, W., A. Salih Mohammed, R. Kurda, K. Ghafor, L. Cavaleri, S. M. A., Qaidi, et al. Prediction of concrete materials compressive

- strength using surrogate models. *Structures*, Vol. 46, 2022, pp. 1243–1267.
- [25] Shakr Piro, N., A. Mohammed, S. M. Hamad, and R. Kurda. Electrical resistivity-Compressive strength predictions for normal strength concrete with waste steel slag as a coarse aggregate replacement using various analytical models. *Construction and Building Materials*, Vol. 327, 2022, id. 127008.
- [26] Alves Ribeiro, V. H. and G. Reynoso-Meza. Ensemble learning by means of a multi-objective optimization design approach for dealing with imbalanced data sets. *Expert Systems With Applications*, Vol. 147, 2020, id. 113232.
- [27] Oyeyi, A. G., A. Khan, J. Huyan, W. Zhang, F. M. W. Ni, and S. L. Tighe. Ensemble and evolutionary prediction of layers temperature in conventional and lightweight cellular concrete subbase pavements. *International Journal of Pavement Engineering*, Vol. 25, 2024, id. 2322525.
- [28] Khan, A., J. Huyan, R. Zhang, Y. Zhu, W. Zhang, G. Ying, et al. An ensemble tree-based prediction of Marshall mix design parameters and resilient modulus in stabilized base materials. Construction and Building Materials, Vol. 401, 2023, id. 132833.
- [29] Lyngdoh, G. A., M. Zaki, N. M. A. Krishnan, and S. Das. Prediction of concrete strengths enabled by missing data imputation and interpretable machine learning. *Cement and Concrete Composites*, Vol. 128, 2022, id. 104414.
- [30] Pranav, S., M. Lahoti, and M. Gopalarathnam. Concrete compress strength prediction using boosting algorithms, Springer, Singapore, 2023, pp. 307–315.
- [31] Karim, R., M. H. Islam, S. D. Datta, and A. Kashem. Synergistic effects of supplementary cementitious materials and compressive strength prediction of concrete using machine learning algorithms with SHAP and PDP analyses. Case Studies in Construction Materials, Vol. 20, 2024, id. e02828.
- [32] Kashem, A., R. Karim, S. C. Malo, P. Das, S. D. Datta, and M. Alharthai. Hybrid data-driven approaches to predicting the compressive strength of ultra-high-performance concrete using SHAP and PDP analyses. Case Studies in Construction Materials, Vol. 20, 2024, id. e02991.
- [33] Shahmansouri, A. A., H. Akbarzadeh Bengar, and S. Ghanbari. Compressive strength prediction of eco-efficient GGBS-based geopolymer concrete using GEP method. *Journal of Building Engineering*, Vol. 31, 2020, id. 101326.
- [34] Chu, H.-H., M. A. Khan, M. Javed, A. Zafar, M. Ijaz Khan, H. Alabduljabbar, et al. Sustainable use of fly-ash: Use of geneexpression programming (GEP) and multi-expression programming (MEP) for forecasting the compressive strength geopolymer concrete. *Ain Shams Engineering Journal*, Vol. 12, 2021, pp. 3603–3617.
- [35] Kioumarsi, M., H. Dabiri, A. Kandiri, and V. Farhangi. Compressive strength of concrete containing furnace blast slag; optimized machine learning-based models. Cleaner Engineering and Technology, Vol. 13, 2023, id. 100604.
- [36] Ray, S., M. M. Rahman, M. Haque, M. W. Hasan, and M. M. Alam. Performance evaluation of SVM and GBM in predicting compressive and splitting tensile strength of concrete prepared with ceramic waste and nylon fiber. *Journal of King Saud University*, Vol. 35, 2023, pp. 92–100.
- [37] Saha, P., P. Debnath, and P. Thomas. Prediction of fresh and hardened properties of self-compacting concrete using support vector regression approach. *Neural Computing & Applications*, Vol. 32, 2020, pp. 7995–8010.

[38] Naser, A. H., A. H. Badr, S. N. Henedy, K. A. Ostrowski, and H. Imran. Application of Multivariate Adaptive Regression Splines (MARS) approach in prediction of compressive strength of eco-friendly concrete. Case Studies in Construction Materials, Vol. 17, 2022, id. e01262.

**DE GRUYTER** 

- [39] Amin, M. N., A. A. A. Al-Naghi, R.-U.-D. Nassar, O. Algassem, S. A. Khan, and A. F. Deifalla. Investigating the rheological characteristics of alkali-activated concrete using contemporary artificial intelligence approaches. Reviews on Advanced Materials Science, Vol. 63, 2024, id. 20240006.
- [40] Amin, M. N., S. A. Khan, A. A. Alawi Al-Naghi, E. R. Latifee, N. Alnawmasi, and A. F. Deifalla. Low-carbon embodied alkaliactivated materials for sustainable construction: A comparative study of single and ensemble learners. Reviews on Advanced Materials Science, Vol. 63, 2024, id. 20230162.
- [41] Ashrafian, A., E. Panahi, S. Salehi, M. Karoglou, and P. G. Asteris. Mapping the strength of agro-ecological lightweight concrete containing oil palm by-product using artificial intelligence techniques. Structures, Vol. 48, 2023, pp. 1209-1229.
- [42] Yang, J., P. Jiang, R.-U.-D. Nassar, S. A. Suhail, M. Sufian, and A. F. Deifalla. Experimental investigation and AI prediction modelling of ceramic waste powder concrete - An approach towards sustainable construction. Journal of Materials Research and Technology, Vol. 23, 2023, pp. 3676-3696.
- [43] Bušić, R., M. Benšić, I. Miličević, and K. Strukar. Prediction models for the mechanical properties of self-compacting concrete with recycled rubber and silica fume. Materials, Vol. 13, 2020, id. 1821.
- [44] Mehta, V. Machine learning approach for predicting concrete compressive, splitting tensile, and flexural strength with waste foundry sand. Journal of Building Engineering, Vol. 70, 2023, id. 106363.
- [45] Golafshani, E. M. and A. Behnood. Predicting the mechanical properties of sustainable concrete containing waste foundry sand using multi-objective ANN approach. Construction and Building Materials, Vol. 291, 2021, id. 123314.
- [46] Ali, R., M. Muayad, A. S. Mohammed, and P. G. Asteris. Analysis and prediction of the effect of Nanosilica on the compressive strength of concrete with different mix proportions and specimen sizes using various numerical approaches. Structural Concrete, Vol. 24, 2023, pp. 4161-4184.
- [47] Kashem, A., R. Karim, P. Das, S. D. Datta, and M. Alharthai. Compressive strength prediction of sustainable concrete incorporating rice husk ash (RHA) using hybrid machine learning algorithms and parametric analyses. Case Studies in Construction Materials, Vol. 20, 2024, id. e03030.
- [48] Kakasor Ismael Jaf, D., P. Ismael Abdulrahman, A. Salih Mohammed, R. Kurda, S. M. A. Qaidi, and P. G. Asteris. Machine learning techniques and multi-scale models to evaluate the impact of silicon dioxide (SiO2) and calcium oxide (CaO) in fly ash on the compressive strength of green concrete. Construction and Building Materials, Vol. 400, 2023, id. 132604.
- [49] Mohammed, A., R. Kurda, D. J. Armaghani, and M. Hasanipanah. Prediction of compressive strength of concrete modified with fly ash: applications of neuro-swarm and neuro-imperialism models. Computers and Concrete, Vol. 27, 2021, pp. 489-512.
- [50] Noaman, M. A., M. R. Karim, and M. N. Islam. Comparative study of pozzolanic and filler effect of rice husk ash on the mechanical properties and microstructure of brick aggregate concrete. Heliyon, Vol. 5, 2019, id. e01926.

- [51] Ameri, F., P. Shoaei, N. Bahrami, M. Vaezi, and T. Ozbakkaloglu. Optimum rice husk ash content and bacterial concentration in selfcompacting concrete. Construction and Building Materials, Vol. 222, 2019, pp. 796-813.
- [52] Rajashekhar Reddy, K., M. Harihanandh, and K. Murali. Strength performance of high-grade concrete using rice husk ash (RHA) as cement replacement material. Materials Today: Proceedings, Vol. 46, 2021, pp. 8822-8825.
- [53] Zareei, S. A., F. Ameri, F. Dorostkar, and M. Ahmadi. Rice husk ash as a partial replacement of cement in high strength concrete containing micro silica: Evaluating durability and mechanical properties. Case Studies in Construction Materials, Vol. 7, 2017, pp. 73-81.
- [54] Olutoge, F. A. and P. A. Adesina. Effects of rice husk ash prepared from charcoal-powered incinerator on the strength and durability properties of concrete. Construction and Building Materials, Vol. 196, 2019, pp. 386-394.
- [55] Krishna, N. K., S. Sandeep, and K. M. Mini. Study on concrete with partial replacement of cement by rice husk ash. IOP Conference Series: Materials Science and Engineering, Vol. 149, 2016, id. 012109.
- [56] Amin, M. and B. A. Abdelsalam. Efficiency of rice husk ash and fly ash as reactivity materials in sustainable concrete. Sustainable Environment Research, Vol. 29, 2019, id. 30.
- Ganesan, K., K. Rajagopal, and K. Thangavel. Rice husk ash blended [57] cement: Assessment of optimal level of replacement for strength and permeability properties of concrete. Construction and Building Materials, Vol. 22, 2008, pp. 1675-1683.
- [58] Gautam, A., R. Batra, and N. Singh. A study on use of rice husk ash in concrete. Engineering Heritage Journal, Vol. 3, 2019, pp. 01-04.
- Ahmed, S. O. Rice husk ash as a partial replacement of cement in [59] high strength concrete containing fly ash. International Journal of Current Engineering and Technology, Vol. 11, 2021, pp. 195–200.
- [60] Breiman, L. Random forests. Machine Learning, Vol. 45, 2001, pp. 5-32.
- [61] Milad, A., S. H. Hussein, A. R. Khekan, M. Rashid, H. Al-Msari, and T. H. Tran. Development of ensemble machine learning approaches for designing fiber-reinforced polymer composite strain prediction model. Engineering Computation, Vol. 38, 2022, pp. 3625–3637.
- [62] Vapnik, V. N. The nature of statistical learning theory, Springer, New York, 2000.
- [63] Cortes, C. and V. Vapnik, Support-vector networks, Machine Learning, Vol. 20, 1995, pp. 273-297.
- [64] Zhang, W., A. Khan, J. Huyan, J. Zhong, T. Peng, and H. Cheng. Predicting marshall parameters of flexible pavement using support vector machine and genetic programming. Construction and Building Materials, Vol. 306, 2021, id. 124924.
- [65] Kaloop, M. R., D. Kumar, P. Samui, J. W. Hu, and D. Kim. Compressive strength prediction of high-performance concrete using gradient tree boosting machine. Construction and Building Materials, Vol. 264, 2020, id. 120198.
- [66] Gong, M., Y. Bai, J. Qin, J. Wang, P. Yang, and S. Wang. Gradient boosting machine for predicting return temperature of district heating system: A case study for residential buildings in Tianjin. Journal of Building Engineering, Vol. 27, 2020, id. 100950.
- [67] Ferreira, C. Gene Expression Programming: a New Adaptive Algorithm for Solving Problems, Complex Systems, Vol. 13, No. 2, 2001, pp. 87-129.
- Hossein Alavi, A. and A. Hossein Gandomi. A robust data mining approach for formulation of geotechnical engineering systems. Engineering Computations, Vol. 28, 2011, pp. 242-274.

- [69] Shah, H. A., S. K. U. Rehman, M. F. Javed, and Y. Iftikhar. Prediction of compressive and splitting tensile strength of concrete with fly ash by using gene expression programming. *Structural Concrete*, Vol. 23, 2022, pp. 2435–2449.
- [70] Iqbal, M. F., Q. Liu, I. Azim, X. Zhu, J. Yang, M. F. Javed, et al. Prediction of mechanical properties of green concrete incorporating waste foundry sand based on gene expression programming. *Journal of Hazardous Materials*, Vol. 384, 2020, id. 121322.
- [71] Wu, W., Y. Xia, and W. Jin. Predicting bus passenger flow and prioritizing influential factors using multi-source data: scaled stacking gradient boosting decision trees. *IEEE Transactions on Intelligent Transportation Systems*, Vol. 22, 2021, pp. 2510–2523.
- [72] Zhou, Z.-H. Ensemble Methods, Chapman and Hall/CRC, Boca Raton, Florida. USA. 2012.
- [73] Ekanayake, I. U., D. P. P. Meddage, and U. Rathnayake. A novel approach to explain the black-box nature of machine learning in compressive strength predictions of concrete using Shapley additive explanations (SHAP). Case Studies in Construction Materials, Vol. 16, 2022, id. e01059.
- [74] Lundberg, S. M., S.-I. Lee. A unified approach to interpreting model predictions. In *Proceedings of the 31st International Conference on*

- Neural Information Processing Systems (NIPS'17). Curran Associates Inc., Red Hook, NY, USA, 2017, pp. 4768–4777.
- [75] Gandomi, A. H. and D. A. Roke. Assessment of artificial neural network and genetic programming as predictive tools. *Advances in Engineering Software*, Vol. 88, 2015, pp. 63–72.
- [76] Al-Alwan, A. A. K., M. Al-Bazoon, F. I. Mussa, H. A. Alalwan, M. Hatem Shadhar, M. M. Mohammed, et al. The impact of using rice husk ash as a replacement material in concrete: An experimental study. *Journal of King Saud University Engineering Sciences*, 2022.
- [77] Golbraikh, A. and A. Tropsha. Beware of q2! *Journal of Molecular Graphics & Modelling*, Vol. 20, 2002, pp. 269–276.
- [78] Roy, P. P. and K. Roy. On some aspects of variable selection for partial least squares regression models. QSAR & Combinatorial Science, Vol. 27, 2008, pp. 302–313.
- [79] Iftikhar, B., S. C. Alih, M. Vafaei, M. A. Elkotb, M. Shutaywi, M. F. Javed, et al. Predictive modeling of compressive strength of sustainable rice husk ash concrete: Ensemble learner optimization and comparison. *Journal of Cleaner Production*, Vol. 348, 2022, id. 131285.